Research Square

Preprints are preliminary reports that have not undergone peer review.
They should not be considered conclusive, used to inform clinical practice,
or referenced by the media as validated information.

Lower Limb Response to Anti-personnel Landmine Blast Explosions: Injury Assessment and Mitigation Strategies

Baljinder Singh (baljinderkularsingh701@gmail.com)
Indian Institute of Technology Delhi
Mohammad Ahmed Basri
Indian Institute of Technology Delhi

Research Article

Keywords: Blast Injury biomechanics, Lower extremity, Landmine blast, High strain rate, Blast mitigation, Energy Absorption

Posted Date: June 23rd, 2022

DOI: https://doi.org/10.21203/rs.3.rs-1765590/v1

License: This work is licensed under a Creative Commons Attribution 4.0 International License.
Read Full License

Lower Limb Response to Anti-personnel Landmine Blast Explosions: Injury Assessment and Mitigation Strategies

Baljinder Singh[1*], Mohammad Ahmed Basri[1]

[1]Department of Mechanical Engineering, Indian Institute of Technology Delhi, New Delhi, India
[*]Corresponding Author E-Mail: bskular.singh@gmail.com

Abstract:

Injuries in lower extremities due to anti-personnel (AP) landmine blasts have been a major cause of amputation in soldiers. Therefore, it is crucial to understand the mechanism of these injuries for designing advanced personnel protective equipment and superior medical interventions. Various attempts have been made to correlate lower limb cadaveric mine blast test data using surrogate models, but till date, no study has been reported to validate it using numerical methods. In this work, a finite element computational framework was developed for landmine blasts using a biofidelic human body lower limb model for validating *in situ* tibia forces and injury patterns with PMHS (Post Mortem Human Subjects) test data. Based on the reliability of the validated numerical analysis model, efforts were made to elucidate landmine blast physics, blast wave intensity for various mine threats, pathophysiology of lower extremity trauma, and effectiveness of various blast mitigation strategies. Numerical simulations were performed to assess the level of protection offered by a standard army combat boot to the lower limb for an M-14 mine blast. Furthermore, for attenuating the load transmission to the lower limb, aluminium foam sandwich panel has been proposed as a potential shoe insert material due to its high energy absorption capabilities. Compared to the bare foot scenario, aluminum foam shoe insert in double core configuration was effective in minimizing severity of M-14 mine blast injuries by reducing the peak tibia force by 34% with a significant delay in time of arrival of the peak. Additionally, the proposed mine protective shoe concept offers 25.2% more reduction in peak tibia force compared to the standard military combat boot for a charge triggered by victim's heel.

Keywords: Blast Injury biomechanics, Lower extremity, Landmine blast, High strain rate, Blast mitigation, Energy Absorption

1 Introduction:

Anti-personnel landmine blasts involve direct interaction of high-pressure blast waves with human foot resulting in complex injuries involving musculoskeletal disruption, bone splintering, and heterotopic ossification. These injuries lead to amputations and in some worst scenarios, may even lead to fatalities. Even if the limb is not fully amputated, such injuries have a prolonged effect on the functional mobility thereby affecting the return to duty of military personnel. AP mine blast results in high strain rate failure of lower extremity (LE) biological tissues; however, the current injury data and thresholds are only available from automotive crash tests. Landmine blast loading is reasonably different from impact and anti-vehicle blast in terms of magnitude, rate of loading, and injury pattern, and further in the way the blast wave is reflected and amplified by surrounding mediums. Current information about the biomechanical nature of these injuries is limited by the paucity of landmine blast injury research. Without proper knowledge about the injury physics, it is futile to design the protective equipment. Therefore, for designing effective military personnel protective equipment, it is imperative to develop a high-fidelity model to decipher the lower extremity mine blast response and pathophysiology of mine blast trauma.

In order to evaluate the lower extremity trauma and efficacy of mine protective footwear, various surrogate models have been developed. NATO task group HFM 08/TG-024 [2] classified lower limb surrogate models into three main types (i) mechanical legs for screening (ii) frangible legs for Proofing (iii) Cadavers for validation purposes. Mechanical legs were the first surrogates to be used for mine blast research. For screening the relative performance of protective footwear, low-cost, rigid mechanical leg representing the mass and outer anatomic dimensions of the human leg would suffice. Coffey et al. at Defense Research and Development Canada (DRDC) constructed a mechanical leg with accelerometers and strain gauge mounted on an Aluminum tubing, a polymeric calf flesh and foot [3]. The Netherlands Mechanical Leg took a simple metal tube construction for the upper and lower leg connected by a mechanical knee joint. It was later modified to the hybrid III crash test dummy with mounted accelerometers to develop injury criterion for automotive crash investigations [4]. These mechanical legs were essentially rigid and therefore failed to accurately capture the mechanical response of human tissues once the fracture initiates. Frangible surrogate legs (FSL) overcame this limitation by incorporating

biologically similar materials to replicate musculoskeletal fractures. A simplified lower leg (SSL) frangible surrogate was developed by DRDC, having single bones representing the limb surrounded by gelatin soft tissues [5]. SLL was modified to the surrogate complex lower leg (CLL) utilizing polymeric materials with strain rate sensitivity and fracture strength equivalent to biological materials [6]. Australian defense science and technology organization (DSTO) developed a 50th percentile Australian male FSL with anatomically correct representations of human leg bones, tendons, soft tissues, and capable of allowing trauma evaluation by autopsies [7]. Defense R&D Canada, Suffield [8] used the Australian FSL to conduct mine blasts tests, and correlated FSL response and injury patterns with cadaver data [9]. Results indicated that FSL models are stiffer, predict unrealistic tibiae transverse fracture patterns, and lack the fracture sensitivity in talus/calcaneus bones resulting in amplified response parameters. For predicting mine blast response of a lower extremity, there could be nothing better than conducting tests using actual human cadavers that accurately represent human anatomy and material behavior. Till date, only two cadaveric tests have been reported to evaluate the effect of landmine blast on the human lower extremity. U.K researchers examined lower limb trauma with cadavers suspended near the knee location from a test fixture [4]. US department of defense carried out Lower Extremity Assessment Program (LEAP) on full body human cadavers subjected to various levels of threat/protection combination [9]. This study is one of the best documented literatures available for the cadaver forces, injury mechanism, and protective footwear efficacy for different threats/protection combinations. R. Harris et al. then went on to publish seven additional cadaveric studies using M-14 mines reporting the force level, time to peak, impulse, and strains on a human lower limb protected by various boots [10]. However, cadaveric test data in general suffer from experimental inconsistencies and properties degradation due to age and prevailing medical conditions.

The development of novel medical interventions and armors require detailed *in vivo* cadaver studies using real landmines. Cadaveric experiments have legal constraints; require ethical approvals and biomedical expertise, while procuring real landmines is banned by various international treaties ([1]). Surrogate models are in general costly and have limited fidelity in terms of replicating cadaver response and fracture mechanism. Numerical (FE) models are excellent reliable, cost-effective, and time efficient alternative for determining the lower

extremity mine blast trauma. Modelling of a mine blast require accurate representation of soil and detonation products interaction which makes it critical for the soil model to function properly. Bergeron et al [11] conducted tests on detonation of a 100-gram landmine in soil for various charge depths demonstrating mine blast physics and reported various blast parameters. Wang et al. [12] performed a benchmark study on landmine explosions in soil using Arbitrary Eulerian-Lagrangian (ALE) approach and attempted to validate in-soil and air pressure test data from Bergeron et al. [11]. This model served a baseline for mine blast simulations on structures, military vehicles, and human models. However, the test data that was validated had inconsistencies because of charge pliability, leading to reduced correlation between simulated data and test results. Motuz et al. [13] developed a computational framework using the ALE approach for simulating the surrogate single leg (SLL) model for a short duration of 2 microseconds. Numerical predictions were compared with SLL test data [5] and mine blast results [14]. However, Motuz et al. [13] faced challenge in modelling the soil failure criteria to preclude it from carrying tension, which eventually underestimated the pressure values, caused unrealistic soil containment, and path diversion of the detonation products. They reported that their Lagrangian mesh distortion disrupted the analysis prematurely. Fichera et al. [15] correlated Human Body Model (HBM) simulations using the ALE approach with FSL injury data [16]. Response parameters were not reported, and injury profile correlated with FSL was a vague depiction of foot deformation. Bertucci et al [17] used numerical studies to report lower extremity pressure profiles in a mine blast framework. However, results were not validated, and injury patterns presented need significant refinement.

In this current work, numerical predictions were validated for a 100-gram buried mine to develop a reference computational framework for evaluating lower limb mine blast trauma. The computational framework developed, was used to analyze the effect of detonation of M-14 mine under the heel of THUMS^{TM} (Total Human body Model for Safety). M-14 (A.K.A Toe popper) is the world's smallest landmine designed to cause injury to the foot without leading to fatality. The M-14 mine was selected for validation of cadaver experimental data to minimize musculoskeletal strain rate effects in the human tissues. THUMS^{TM} mine blast response was validated with cadaver test data in terms of *in situ* tibia forces and fracture patterns. Additionally, key lower limb injury causing parameters were investigated for four different landmines (M-14

(28gram Tetryl), PMA-3 (35gram Tetryl), PMA-2 (100gram TNT), and PMN (240gram TNT)) to cover the entire threat range of landmine blast. A series of numerical studies were performed to investigate the efficacy of various combination of blast mitigation materials in attenuating the impulse and force transmitted to the lower limb.

2 Methodology

The primary interest of the study is to decipher the interaction between the blast wave and human lower extremity/protective equipment with prime focus on the impulse/energy imparted. The scenario in the air depends on the physics of what happens beneath the ground surface inside the soil. Air blast loads are complicated by the explosion inside soil where the interacting medium undergoes solid, liquid, and gaseous phase changes. Furthermore, studies by [18] suggest that soil focuses and directs the blast wave onto the structures. Therefore, it is critical to understand the in-soil physics for which an initial validation was performed for a 100-gram landmine detonation in soil. Based on the fidelity of the validated mine blast computational framework, THUMS^{TM} was used to validate Lower Extremity Assessment Program (LEAP) cadaveric test studies conducted by the United States Department of Defense [9].

2.1 Model Anatomy and material models

2.1.1 Model Anatomy

For the FE analysis, THUMS^{TM} model is used which is a freeware American 50TH percentile (AM50 pedestrian male version 4.0.2) developed by Toyota central R&D labs and Toyota motor co-corporation in collaboration with Wayne state university, Detroit, Michigan to analyze motor vehicle collision injuries. THUMS^{TM} offers high biofidelity since it uses exact human anatomy, biologically similar materials, and has its biomechanical response corroborated with component level and full body tests [[19], [20], [21], [22], [23]]. The model has mesh size (3-5mm) optimized as per the best available industry standards, and involves intricate modeling of bones, tendons, soft tissues, and ligaments. Details of model anatomy is portrayed in Fig. 1.

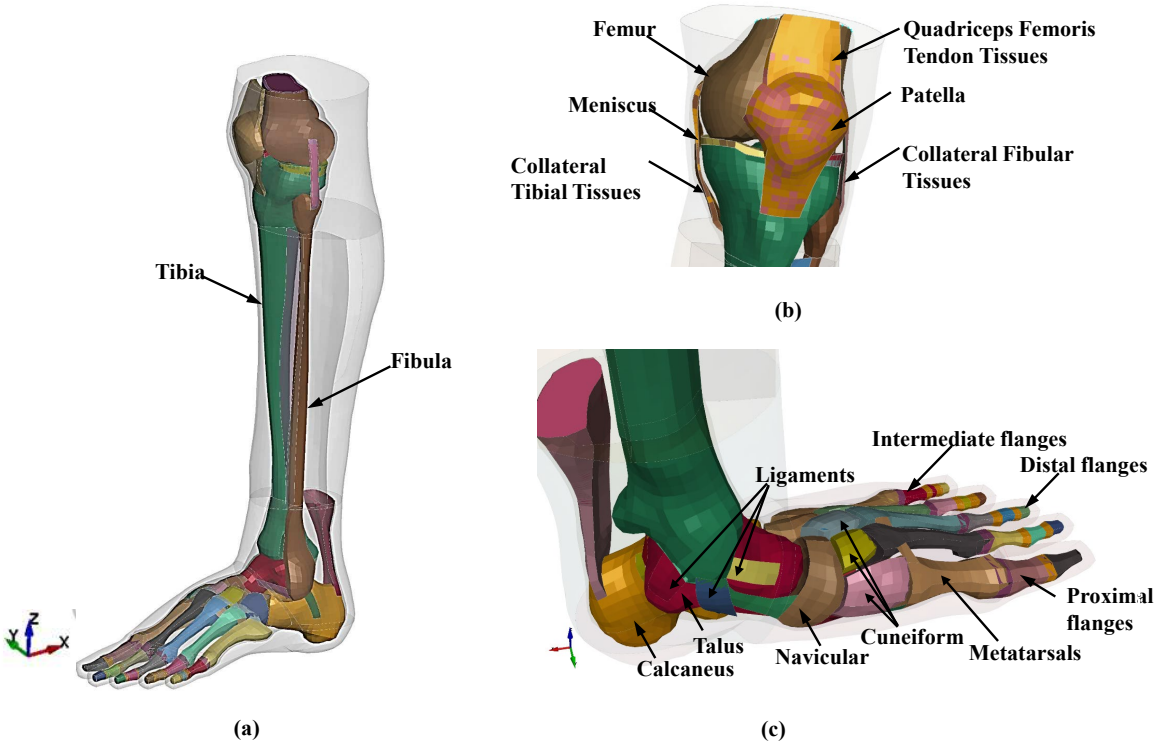

Fig. 1 THUMS^{TM} showing details of (a) lower extremity anatomy, (b) knee joint and (c) foot

2.1.2 Mathematical Material Models

Since THUMS^{TM} was initially developed for pedestrian impact scenario, it was modified to ensure sufficient biofidelity in high strain rate regime of mine blast loading. In THUMS^{TM}, the skeletal parts are assumed non-linear elasto-plastic defined using LS Dyna Mat_Piecewise_Linear_ Plasticity card. Bones are found to exhibit viscoelastic [24], viscoplastic effects [25] at extremely high strain rates resulting in increased strength and brittleness (reduced failure strain). To accurately predict the biomechanical response of bones at high loading rate, a fully viscoplastic (VP) strain rate formulation was applied which incorporates Cowper Symonds law within the yield surface. Use of VP rate effects amounts to additional costs but leads to substantial improvement in computational results [26]. Mathematical formulation of Cowper Symonds law for yield stress scaling is presented below [26]:

$$\sigma_y\left(\varepsilon^{p}_{eff}, \dot{\varepsilon}^{p}_{eff}\right) = \sigma^{s}_{y}\left(\varepsilon^{p}_{eff}\right) + \sigma_y\left(\dot{\varepsilon}\frac{p}{C}_{eff}\right)^{1/P} \quad (1)$$

Here, the dynamic yield stress $\sigma_y\left(\varepsilon_{\text{eff}}^{\text{p}}, \dot{\varepsilon}_{\text{eff}}^{\text{p}}\right)$ is defined as a function of static yield stress $\sigma_{\text{y}}^{\text{s}}\left(\varepsilon_{\text{eff}}^{p}\right)$ and initial yield stress σ_y factored by Cowper Symonds rate term. $\varepsilon_{\text{eff}}^{\text{p}}$ is the effective strain, Effective plastic strain rate is detonated by $\dot{\varepsilon}_{\text{eff}}^{\text{p}}$, C and P are Cowper Symonds constants. The failure criteria for fracture of bones is invoked when local FEM strain reaches the critical threshold values.

2.2 Computational Framework validation

2.2.1 Validation of a 100gram buried mine

An FE computational framework was developed to validate the response parameters for the detonation of a 100 gram mine buried in soil. Defense Research Establishment Suffield [14] conducted experiments on 100 gram C-4 mine detonated at various burial depths (0, 30 and 80mm) to study the mine blast physics. Tests setup depicted in Fig. 2 (a) includes a C-4 mine buried in a dry silica sand filled steel cylinder, apparatus to mount Endevco 8530 series pressure transducers for measuring in-air pressures at different standoff distances, and cheap carbon resistance gauges (CRG) placed in soil to measure blast wave overpressures at very close-field damage prone locations.

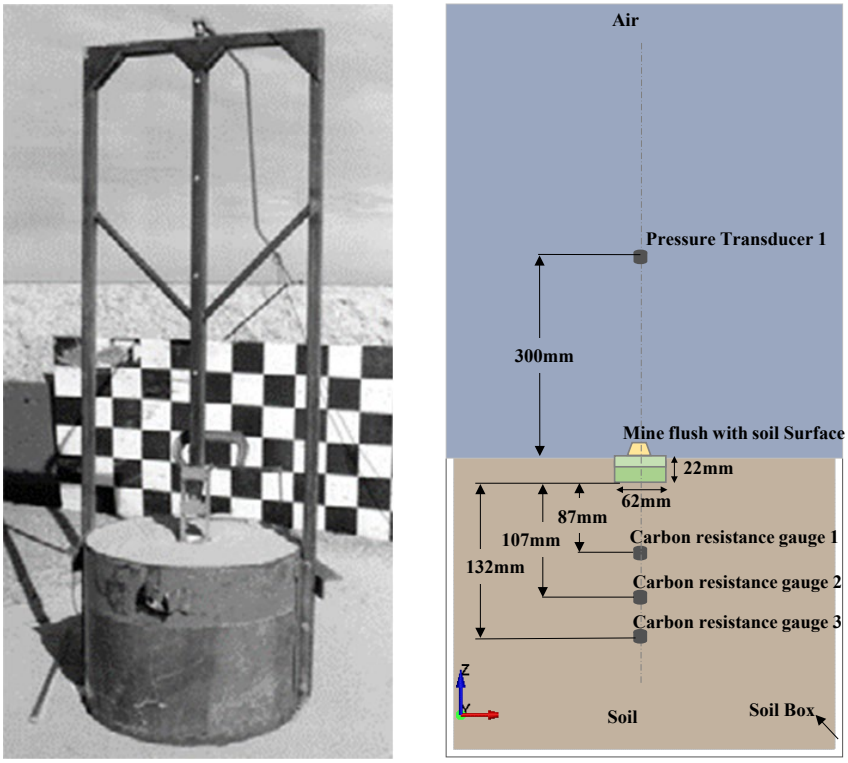

Fig. 2 (a) Experimental set-up, 100-gram AP landmine charge [14] (b) FE model of 100gram C-4 landmine flush with the soil surface illustrating location of in-soil and in-air pressure transducer

Bergeron et al. [14] conducted Series-1 tests by manually placing C-4 charge in a metal mould, due to which the charge became pliable resulting in inaccurate pressure predictions. Also relative larger detonator size compared to the charge height created a venting channel which adversely affected the ejecta pattern. Series-2 tests were then conducted to address the issues encountered in series-1 tests using a thin walled delrin plastic container. Till now, researchers [12] have attempted to validate the series-1 tests with considerably high error margins. Benchmark study for mine blast by Wang J et al. [12] attempted to validate in-air pressures at 300mm above the soil for 30mm depth of burial (DOB) with a minimum error margin of 55%. For the context of this study, Peak overpressures and time of arrival are validated with series 2 test data for three charge burial depths (0mm, 30mm and 80mm). Fig. 2 (b) shows the simulation setup used to replicate test conditions. The locations of in-air (Transducer 1) and in-soil (Carbon resistance gage 1, 2, and 3) pressure transducers to measure the mine blast response parameters are also shown in the Fig. 2 (b).

Dry soil has been modeled with failure using LS dyna *MAT_SOIL_AND_FOAM_FAILURE card [28] and material data for representing air, soil and C-4 explosive are taken from a benchmark simulation study [12]. Time evolution of crater width and height of the blast detonation cloud was compared with experimental data for different mine burial depths and results are collectively presented in Fig. 3. Results indicate that computational framework can capture the soil early deformation and fracture with considerable accuracy (error margin below 5%). This is particularly important since the soil directs and vents the detonation products on lower limb/protective structures in the air. By accurately predicting the soil crater dimenstions, one can accurately estimate the amount of blast wave interacting with the structure.

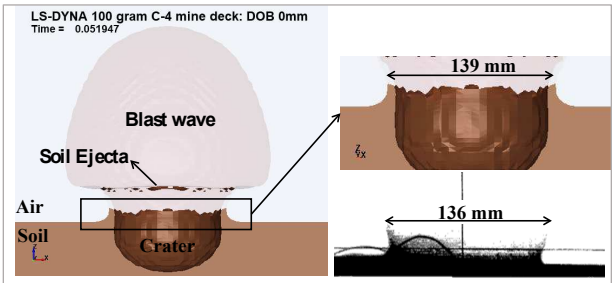

(a) Shot 20-2: 0.051ms 0mm DOB

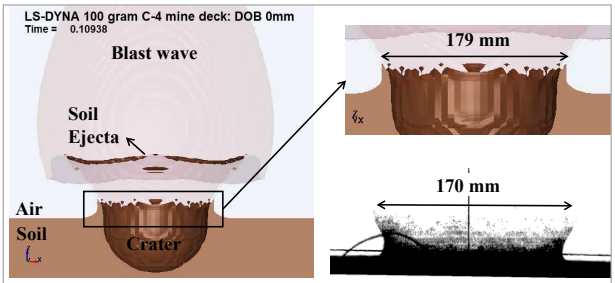

(b) Shot 19-2: 0.102ms 0mm DOB

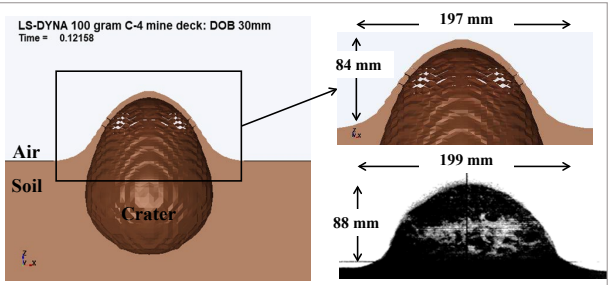

(c) Shot 17-1: 0.126ms 30mm DOB

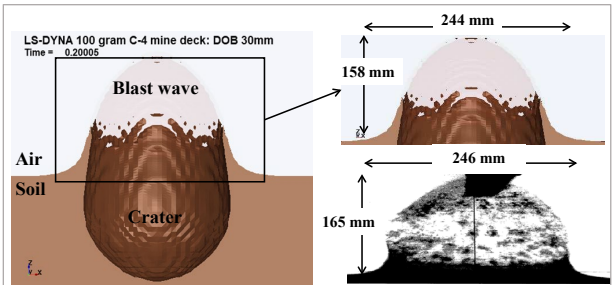

(d) Shot 17-2: 0.201ms 30mm DOB

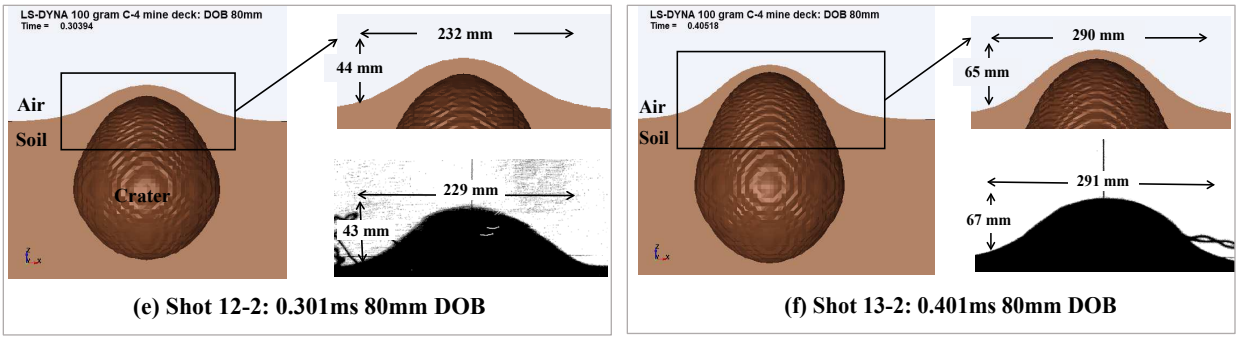

Fig. 3 Time lapse of soil deformation and detonation products expansion in a AP mine blast depicting comparison between experimental [14] and numerically model predicted results in terms of crater and detonation cloud height for (a) Shot 20-2: 0.051ms 0mm DOB (b) Shot 19-2: 0.102ms 0mm DOB (c) Shot 17-1: 0.126ms 30mm DOB (d) Shot 17-2: 0.201ms 30mm DOB (e) Shot 12-2: 0.301ms 80mm DOB (f) Shot 13-2: 0.401ms 80mm DOB

Comparison between the numerically predicted and test results in terms of peak overpressure versus time are presented in Fig. 4 - Fig. 6. Pressure vs time output was filtered using Butterworth filter at a frequency of 1MHz consistent with the data sampling method used in the experiments [14].

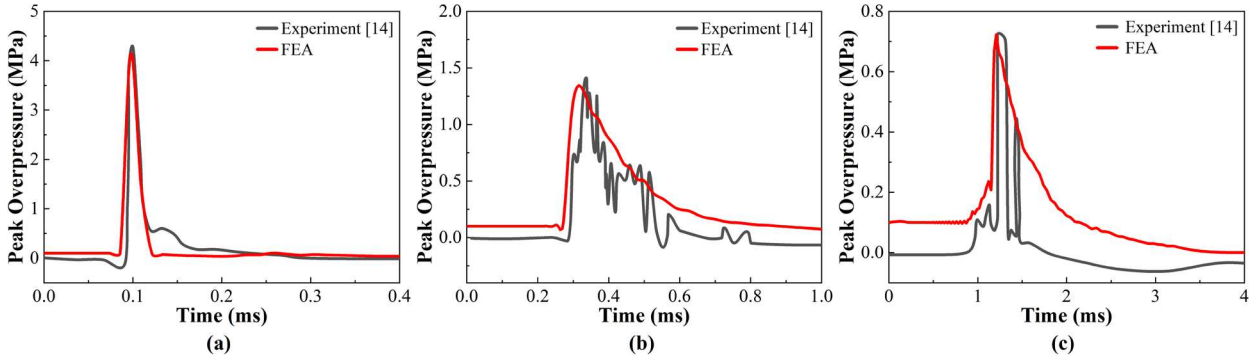

Fig. 4 Comparison between experimental [14] and FE results in terms of Peak in-Air pressures at standoff of 300mm above soil surface for the case of depth of burial (DOB) of (a) 0 mm (b) 30 mm and (c) 80 mm.

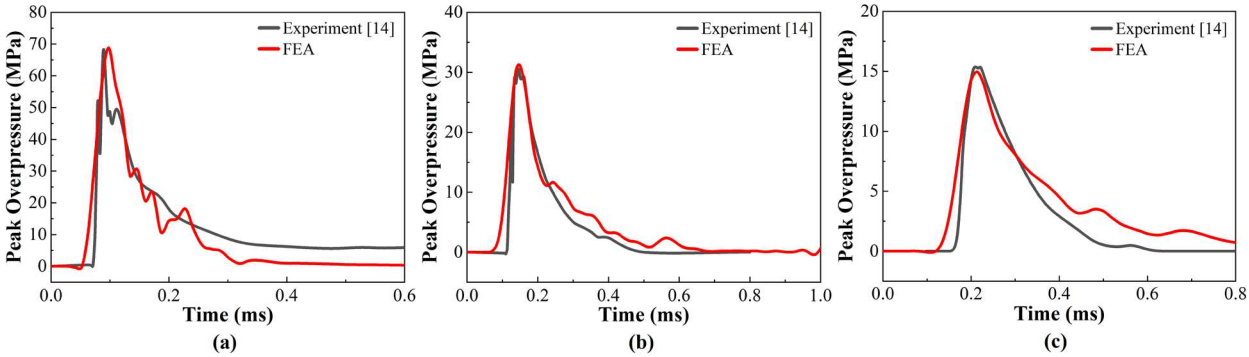

Fig. 5 Comparison between experimental [14] and FE results in terms of in-soil Peak overpressures at standoff of (a) 87.3mm (b) 107.3mm and (c) 132.3mm below the mine with depth of burial (DOB) of 0mm.

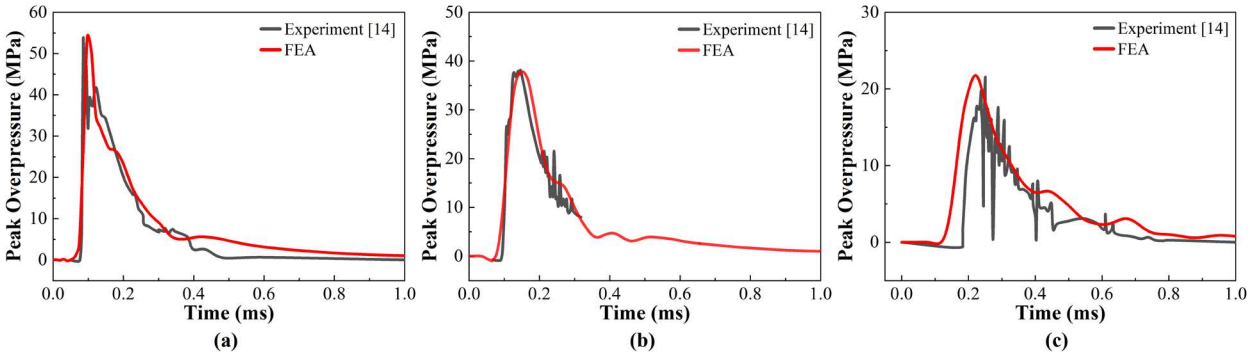

Fig. 6 Comparison between experimental [14] and FE results in terms of in-soil Peak overpressures at standoff of (a) 87.3mm (b) 107.3mm and (c) 132.3mm below the mine with depth of burial (DOB) of 30mm.

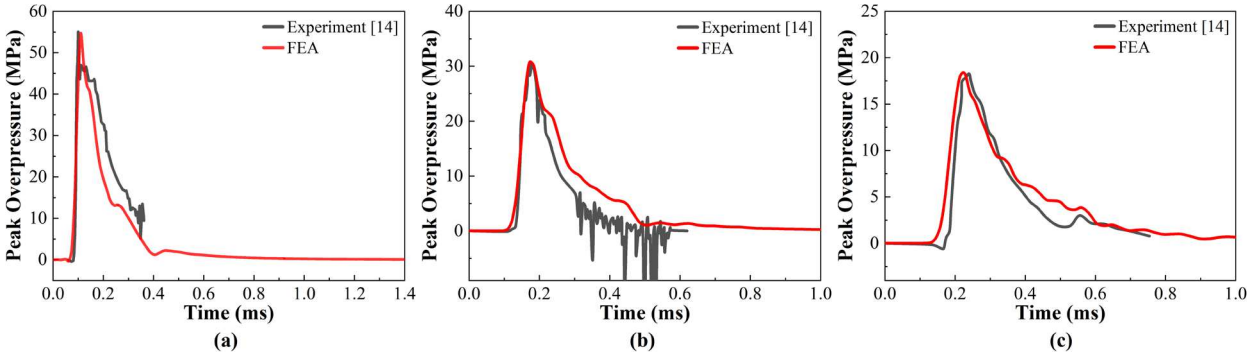

Fig. 7 Comparison between experimental [14] and FE results in terms of in-soil Peak overpressures at standoff of (a) 87.3mm (b) 107.3mm and (c) 132.3mm below the mine with depth of burial (DOB) of 80mm.

Test correlation for in-air overpressures reduced as the soil overburden increased and the highest correlation was obtained for the shock wave induced in-air pressures for the case of DOB=0mm. For a free air blast scenario (no reflections from soil or structures), various simulations studies [29], [30] have concluded that at scaled distance less than 0.25m/kg$^{1/3}$, numerically calculated close field peak overpressures and impulses are significantly higher than proposed by Kingery Bulmash empirical equations [31]. This phenomenon was attributed to complex close field interactions including violent ejection of high-speed detonation products, afterburning, and damage to the transducers very close to the center of the blast. In this study, however, excellent correlation has been achieved for the in-soil CRG's pressures at just 87.3 mm below the mine which corresponds to a near field scaled distance of 0.19m/kg$^{1/3}$. The validated computational framework is thus able to reasonably capture the phenomenon complexities associated with high strain rates effects and near field mine blast physics and is considered accurate enough to study the near field interactions with human lower extremity/ protective equipment.

2.2.2 Lower extremity tibia force and fracture response validation

Harris et al. at U.S. Army Institute of Surgical Research (USAISR) conducted lower extremity assesssment program (LEAP) to assess the cadaver injuries and protection levels offered by various mine protective footwear [9]. Test set up involved an 18"x24"x24" rectangular steel box containing dry sand with a mine flush with the soil surface. As shown in Fig. 8, full human cadavers suspended by harnesses from the ceiling, were positioned such that heel is laid directly over the center of the mine in line with the tibia with sufficient body weight to detonate it. Load cell was implanted on tibia mid shaft, and strain gauges were installed on tibia distal medial and calcaneus inner surface. Injury evaluation was carried out by studying post-test clinical radiographs and post clinical dissection findings by certified military orthopedic traumatologists.

Fig. 8 Left: LEAP experimental setup reproduced by Bergeron et al. [16] Land mine buried flush with the soil surface at center of soil container, Right: Vertical alignment of the model with the heel positioned over the land mine

FE model was used to replicate the test conditions by importing THUMS^{TM} in the mine blast computational framework validated in section 2.2.1 with its heel placed directly over the M-14 mine. Attempt was made to compare the tibia axial force in simulations with experimental values for two series of test studies. One with an M-14 mine detonation under heel of an improvised footwear/tire sandal from LEAP studies [9], the second test involved Leap pilot study with M-14 mine detonation under heel of a combat boot [10]. For validating the cadaver test data, lower extremity FE model was fine tuned to match the test configuration as closely as possible. Lower extremity was extracted from the THUMS^{TM} model and ballast inertia was applied on top of the lower extremity to account for the upper body. Load cell was modelled as a dependent node between two rigid constrained_interpolation (RBE3) elements representing the metallic load cell structure by removing a 102mm segment from proximal tibia. Weight of the load cell has been applied as a concentrated mass at the dependent node of the RBE3 (centroid of the removed segment), as the weight of the load cell might play a role in altering the actual value of force at that section. Combat boot was modelled based on the measurements from computed tomography (CT) scans and dynamic, uniaxial compression tests on Meindl desert fox combat boot, validated for an anti-vehicle (AV) blast scenario [32]. Fig. 9 shows the numerical model used to validate the LEAP pilot study [10] depicting combat boot details with defeatured sole grip features to

avoid negative volume instabilities. Arbitrary Eulerian Lagrangian (ALE) approach was used to accomplish the Fluid Structure Interaction (FSI) between the Lagrangian (Combat boot and lower extremity) and the Eulerian (Tetryl, Soil and Air) parts. Flow-out condition was assigned along the free air boundaries and bottom face of the soil box was restrained in all directions. Cylindrical M-14 mine (Toe popper) was modelled using 28 grams of Tetryl explosive as per its detailed technical drawing [33]. The plastic body of the mine was not modelled and secondary effects caused by mine fragments were neglected. By doing so, only the primary blast wave induced phenomenon was investigated. Even though the M-14 mine is flushed with the soil surface, cylindrical charge is modeled 29 mm below the soil surface, to account for the upper actuating mechanism [33]. Material properties of the Tetryl explosive are taken from [34].

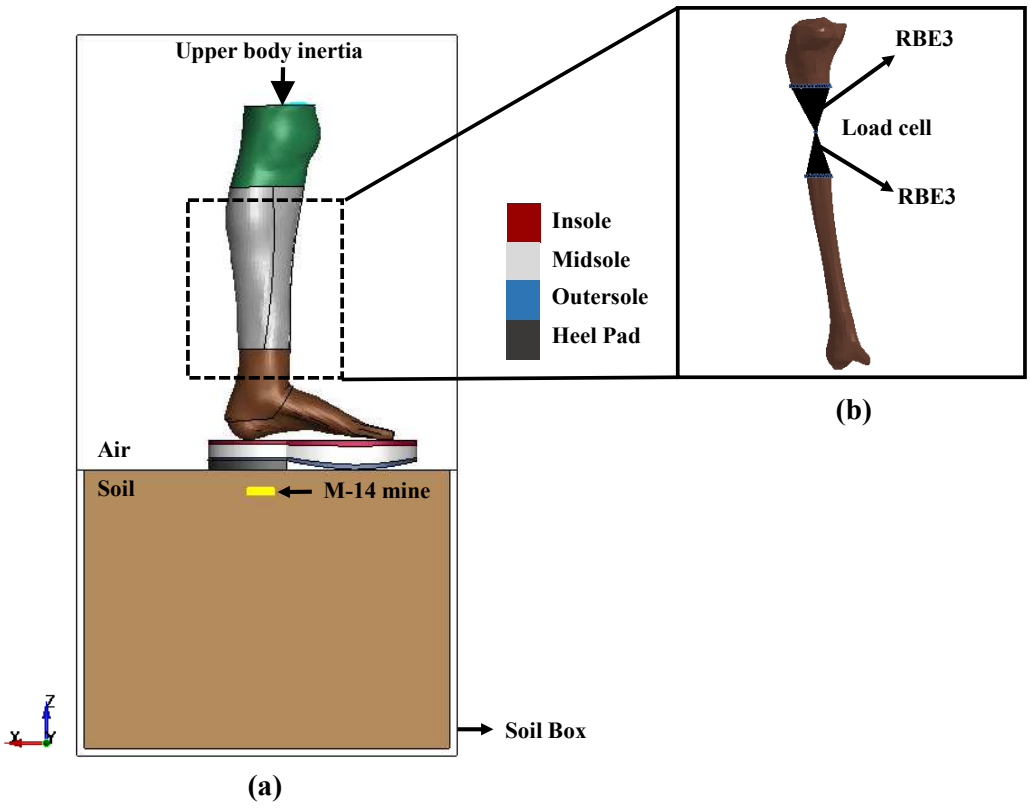

Fig. 9 (a) Sagittal view of the lower extremity depicting details of the FE computational framework for detonation M-14 mine under the heel of the combat boot (b) Load cell representation using rigid interpolation elements [32]

Comparison between the experimental and numerically predicted results of tibia axial force vs time for the case of M-14 mine detonation under an improvised footwear/tire sandal are presented in Fig. 10 (a). Tire sandal offers negligible mitigation to the M-14 mine blast loads and therefore the shot of M-14 mine on tire sandal is modelled as a bare foot scenario. The experimental and numerical results show two prominent peaks in the first case. The numerical analysis is able to predict the first peak with an error margin of 3.3%. The first peak is detrimental for the lower extremity and hence accurate estimation of the first peak is more important. Meindl combat boot was used to validate the pilot study in LEAP carried out using seven M-14 mines, and the correlation between experimental and computational studies for the latter is depicted in Fig. 10 (b). In this case, there is a single prominent peak in the tibia force vs time curve and other peaks are relatively smaller and thus can be ignored. Table 2 summarizes the percentage error between the experimental and numerical results. The results show that the FE results are in good correlation with the experimental in-situ tibia forces for the case of M-14 mine triggered at the location of victim's heel.

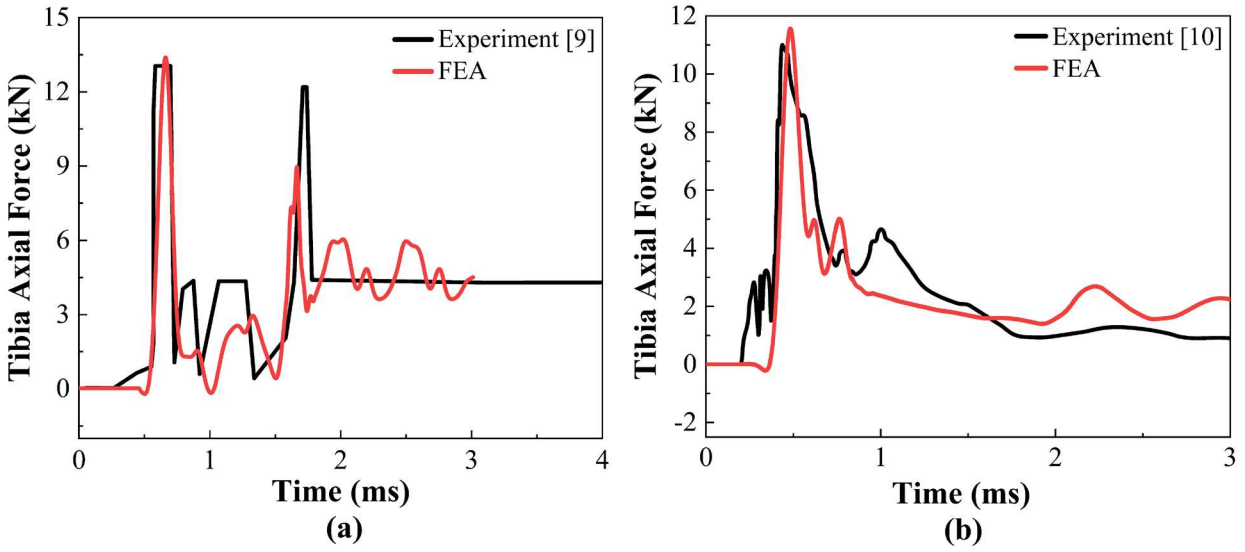

Fig. 10 Comparison between numerically predicted tibia axial loads and the cadaveric test data for the case of M-14 mine detonation under a foot wearing (a) tire sandal [9] and (b) a combat boot [10].

Table 1 Experimental and numerical tibia axial forces

M-14 Shot#	Protection	Experimental tibia axial force (N)	Numerical tibia axial force (N)	Error
26 [9]	Tire sandal	13048	13500	3.3%
Test 6 [10]	Combat boot	11003	11400	3.5%

Fig. 11 shows the injury patterns obtained from FE results for M-14 mine detonation under the heel and its correlation with the cadaveric post test clinical and dissection radiographic findings in the LEAP study (shot 27) [9]. Post test radiography findings reveal a disrupted mid-foot with an intact forefoot and traumatic amputation of 1/3rd of the leg, which is quite evident in FEM model failure predictions. FE results in Fig. 11 shows brisance at calcaneus, talus bones and disruption of chopart and lisfranc joints, which corroborates exactly with autopsy examination of tested cadavers. In FEM, four and fifth metatarsals were disrupted while 1st and 2nd metatarsals fractured in the test data. This small discrepancy might be due orientation of the leg with respect to mine. to left or right.

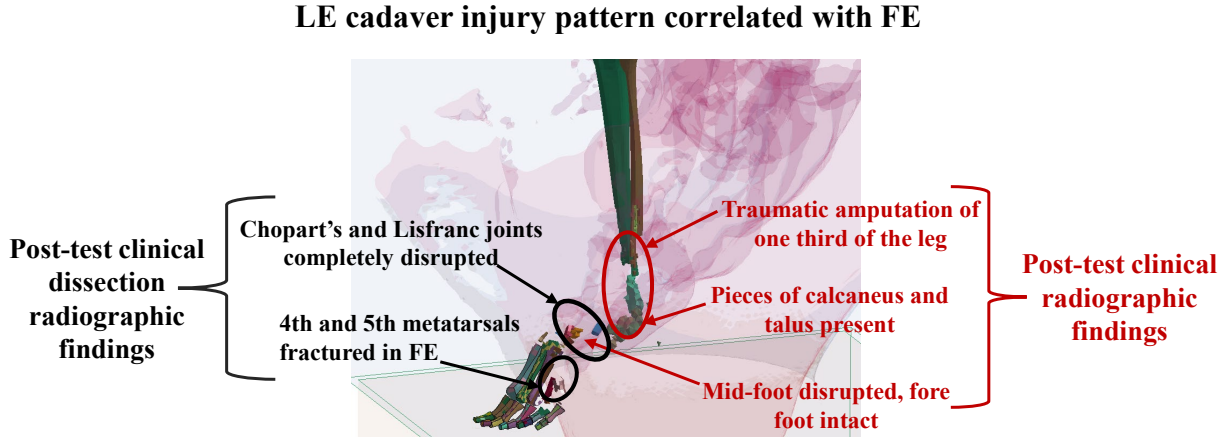

Fig. 11 FEM results correlation with PMHS test findings showing orthopedic injury patterns on the foot for a M-14 mine triggered under the victim's heel [9]

3 Results and discussion

3.1 M-14 mine blast physics

M-14 mine also known as toe popper just maims the foot of the victim and doesn't kill, it is mostly used as a cheap protection of long borders against intruders by many nations. To understand the interaction of the blast wave with the human leg and study the injury pattern, it is important to investigate the mine blast physics (Threat perception). In this section, the mine blast physics of M-14 mine has been discussed based on the validated numerical analysis.

Detonation of a mine within the ground results in energy transmission to the surrounding environment i.e. the ground, air and nearby structures. Some of this energy is dissipated as heat, kinetic energy of air and soil, work done in soil deformation and expansion of detonation products. Several aspects influence the distribution of energy dissipation and the prime intent of the study is to determine the energy/impulse available to be transmitted to the lower extremity/ protective equipment. For shallow buried mine, amount of energy transmitted vertically upwards (compression, shear and rayleigh stress waves) to the human lower limb/protective equipment depends on the overburden depth, standoff distance, soil properties and moisture content. Three distinct phases characterize the phenomenon evolution:

Explosive detonation and early interaction with the soil : Activation of a M-14 mine creates a detonation shock wave converting solid explosive into high pressure (2701MPa), hot gases. At the immediate vicinity of the explosive, there is a zone of crushing (2R to 3R, where R is explosive radius) where pressure and temperature are extremely high such that the blast wave transmision is independent of the physical soil behaviour [14]. From 3R to 6R, there is a plastic deformation zone causing irreversible crushing and collapse of soil volume [14]. Further outwards, there is an elastic zone where reversible soil deformation occurs due to the shock wave onset. The pressure in this stage reduces from 2701MPa to 230MPa in around 0.052 ms as shown in Fig. 12 (a) and (b), creating a vent hole in soil.

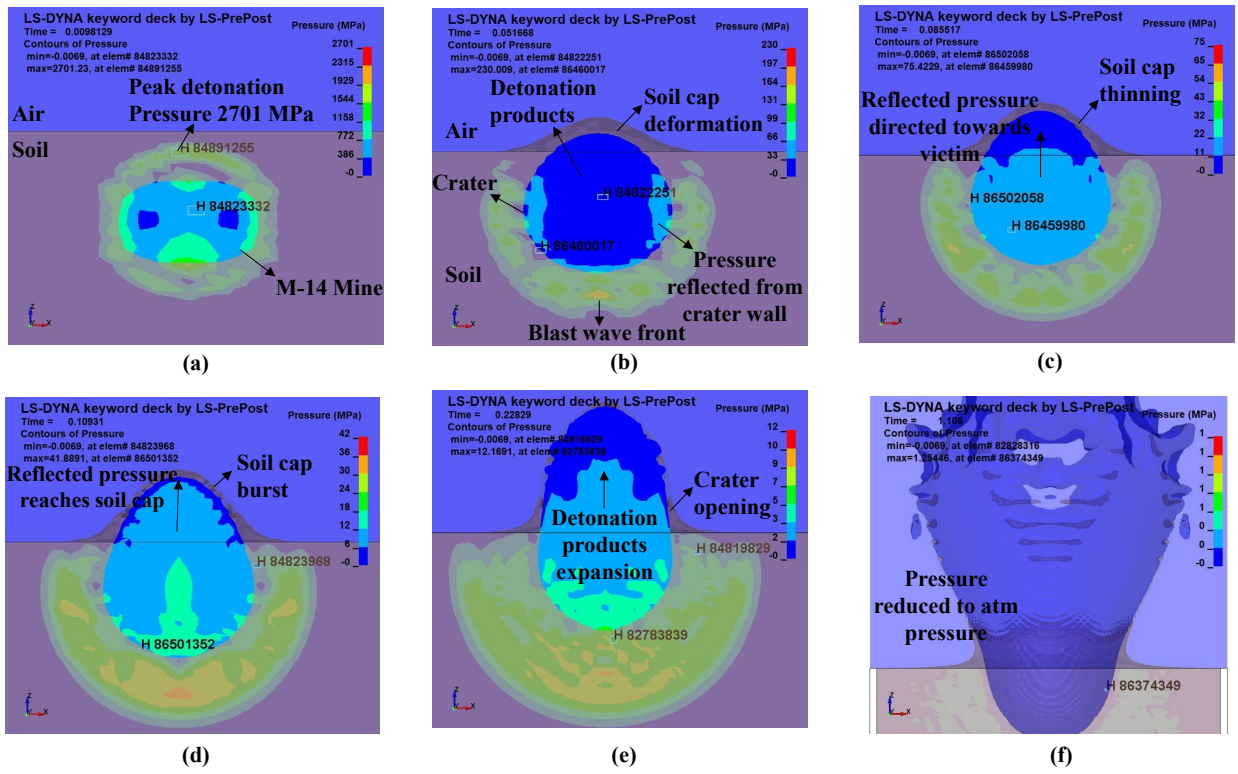

Fig. 12 Physics of M-14 mine blast: depicting the pressure fringe, soil deformation, and movement of detonation products and blast wave (showing locations of maximum and minimum pressures at each instant)

Formation and propagation of the blast wave: Soil being the denser medium contineously directs the detonation products towards the path of least resistance (air), causing deformation at the soil-air interface. As depicted in Fig. 12 (c), pressure fringes reflecting from crater surface coalesces into a pressure wave. When this reflected blast wave reaches the soil-air interface, soil cap bursts and the crater acts as a pressure vessel venting high pressure detonation products vertically upwards towards the victim (Fig. 12 (d)). A complex system of shock and rarefraction waves are established in the crater via continuous reflection of detonation products from the highly compressed soil surface and the process contineous for around 1 millisecond.

Soil Ejecta: During mine blast, soil air interface forms a hemisperical cone, expelling ejecta from the crater at high speeds. Detonation products continue to do work on crater walls, eroding and expelling ejecta at high speeds in a vertical trajectory, within an inverse cone having included angle between 60-90 degrees.

3.2 Parametric study: Effect of charge location on the tibia axial force and LE injury patterns

The validated human body model (THUMS^{TM}) was used to study the effect of mine detonation location on the tibia axial loads and lower extremity injury patterns. For this context, the foot was subdivided into three zones: hind-foot (HF), mid-foot (MF), and the front-foot (FF). Mid-foot zone includes the small cuboid, cuneiform, and navicular bones while the front-foot contains the metatarsals and toe flanges. Hind-foot area includes two important bones: the calcaneus and talus. Their main role is to provide support and transmit load to tibia (the main weight carrying member) of the lower extremity. The most critical bones: calcaneus, talus and tibia are located near the hind-foot. Therefore, the cadaveric tests done during the LEAP study [9], have concentrated on detonating mines under the heel in line with the axis of tibia, considering it as a worst case scenario in terms of traumatic amputation to the lower extremity. Nechaev et al. postulated that anthropometrics and detonation location play a crucial role in dictating the injury outcome, based on clinical warfare experience in Afghanistan [35]. Injury patterns were found to be quite different depending on which part of the foot triggers the mine detonation. Hind-foot detonation had a different medical outcome than detonation under the front part of the foot [35]. This effect would essentially be more pronounced for the M-14 mine, having a smaller zone of hemispherical damage, due to lower explosive content. To quantify the impact of mine detonation location, a series of simulation studies were carried out with M-14 mine triggered under the (a) hind-foot (b) mid-foot and (c) front-foot regions for an intact lower extremity shown in Fig. 13. Modelling artificial equipment like sensors, load cells serve as stress concentration points, and may cause unrealistic local damage and hence have been avoided for this study.

Landmine detonation under the hindfoot results in a direct interaction of the compressive blast wave load with the calcaneus, which is subsequently transmitted vertically upwards to talus and tibia. As shown in Fig. 14 (a), there is a progressive decrease in Z-force values which shows the compressive load transmission from calcaneus to tibia through talus. Calcaneus experience the highest Z-force of 49.5kN while the forces transmitted to talus and tibia are 30.5kN and 13.4kN respectively

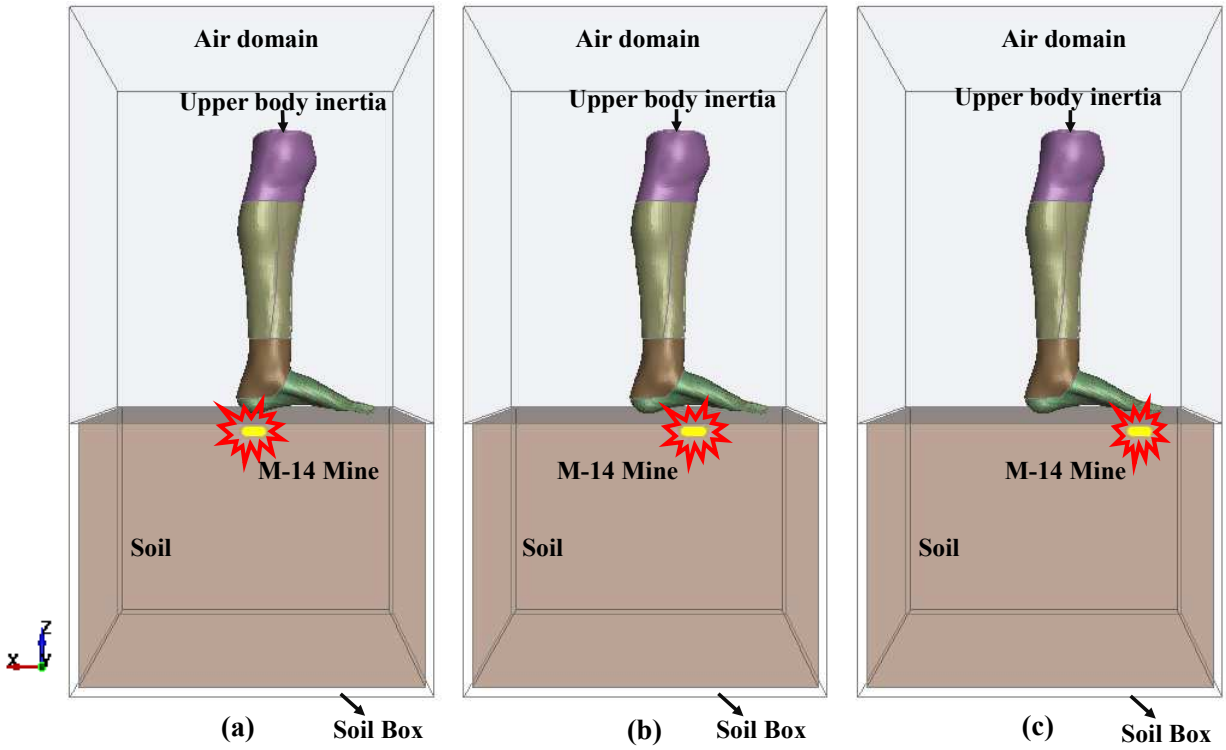

Fig. 13 Finite element model for landmine blast on human lower extremity depicting the M-14 mine detonation locations being investigated on the (a) hind-foot (HF), (b) mid-foot (MF) and (c) front-foot (FF)

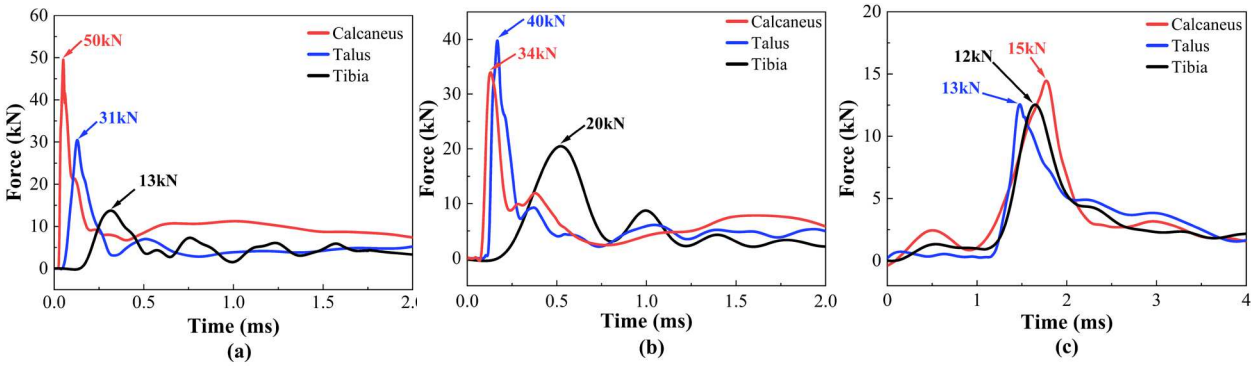

Fig. 14 Forces exerted on the primary foot bones during a (a) Hind-foot (b) Mid-foot and (c) Front-foot detonation of the M-14 mine

Mine triggered by the mid-foot disrupts it, and lateral blast wave impingement tilt and pushes calcaneus posteriorly resulting in a lower Z-force calcaneal force (34kN). Talus however experiences a higher direct Z-force (40kN) due to backward displacement of calcaneus, which in turn is transmitted to tibia (19kN). Mid-foot mine detonation was found to be the most critical scenario with regard to peak forces on talus and tibia. This apparent increase is further supported by the fluid structure interaction (FSI) forces for the three scenarios under investigation. FSI forces depicted in Fig. 15 reveal that FSI loads for mid-foot detonation are around 37% more than the hind-foot scenario.

This is because for hind-foot detonation, most of the charge moves past the heel without any interaction with the foot. Similarly, for mine triggered by the front-foot, a portion of the charge escapes the front of the toe without imparting any impulse to the foot. As shown in Fig. 14 (c), for a front foot detonation, force transmitted to tibia is the lowest and the time of arrival of the peak load is delayed as the blast wave have to travel a larger distance to interact with tibia located towards the hind-foot.

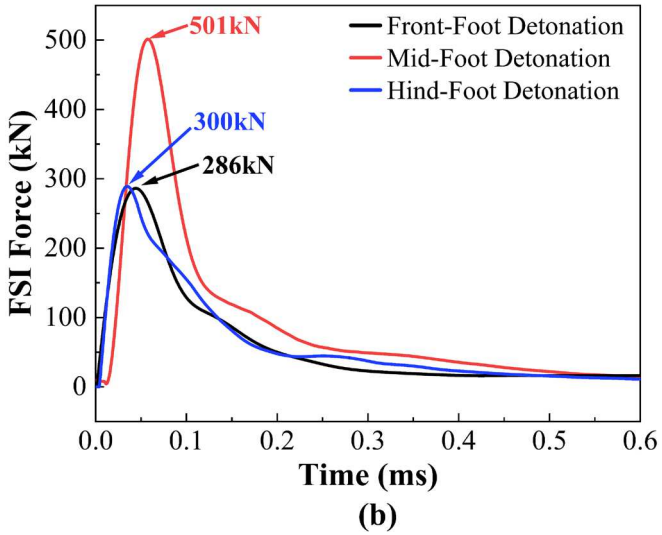

Fig. 15 Comparison of FSI (Fluid Structure Interaction) forces for three detonation locations of the M-14 mine along the human foot

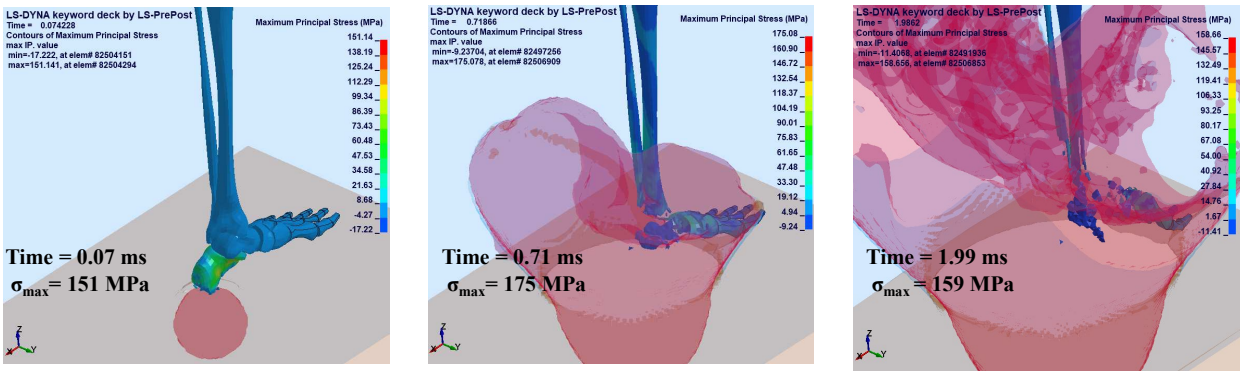

(a) **(b)** **(c)**

Fig. 16 Fringe plots detailing orthopedic lower limb injuries and maximum principal stress distribution fringe plots for M-14 mine detonation under the hind-foot of the victim

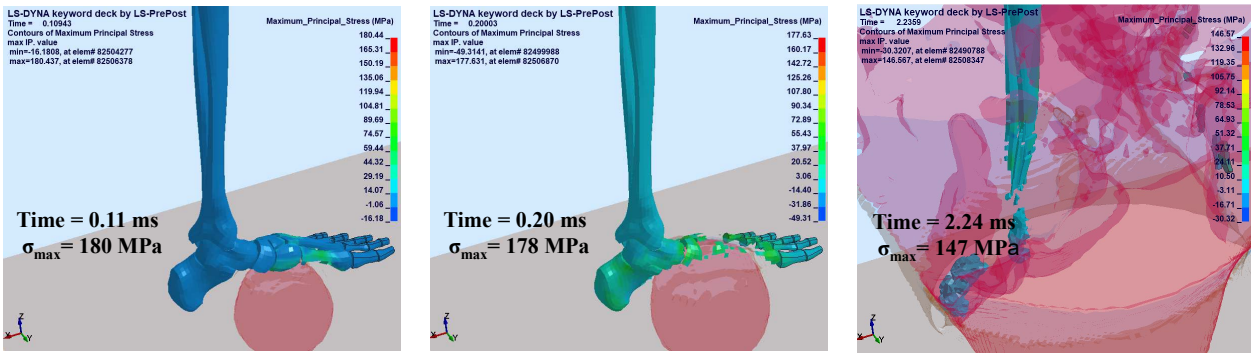

(a) **(b)** **(c)**

Fig. 17 Maximum principal stress distribution fringe plots for the numerical studies run to investigate the orthopedic injuries resulting from M-14 mine detonation under the mid-foot of the victim

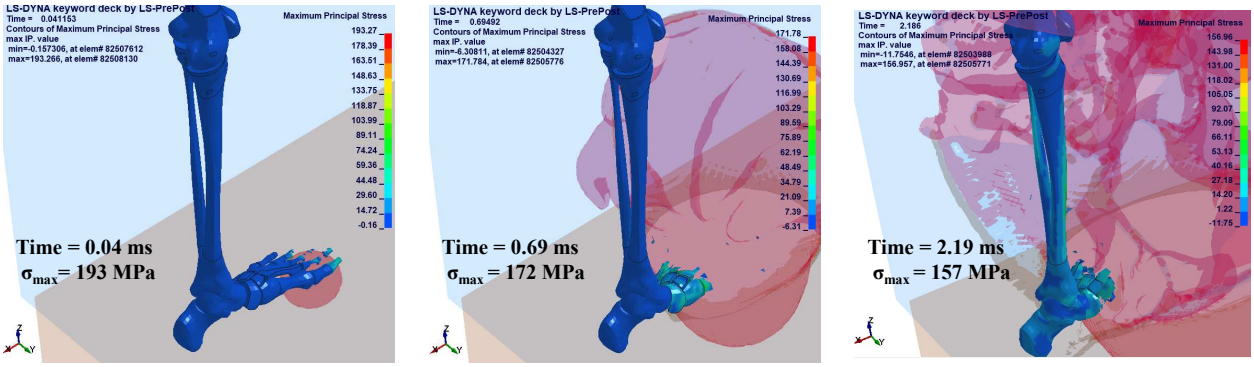

(a) **(b)** **(c)**

Fig. 18 Fringe plots detailing orthopedic lower limb injuries and maximum principal stress distribution fringe plots for M-14 mine detonation under the front-foot of the victim

M-14 mine triggered under the heel results in bone splintering at hind-foot and mid-foot areas, while the front foot remains intact illustrated in Fig. 16. The damage to the lower limb starts distally at calcaneus, located in the immediate vicinity of the mine, and it travels upwards causing brisance of foot bones, and pilon fracture extending to distal end of tibia and fibula. Detonation of M-14 mine under mid-foot offers larger foot area access to the blast wave to incur severe damage, causing comminution of the entire foot as shown in Fig. 17. Charge detonation under the front foot exposes it to such high pressures that bones simply disintegrate resulting in traumatic amputation of the bones at front and mid-foot regions.

3.3 Key lower limb injury causing blast wave parameters across the spectrum of AP mine threats

M-14 mine (discussed in the previous section) is a small AP mine that just decapacitates the victim's foot. In addition to the M-14 mine, other plastic body AP mines also exist which differ in terms of the amount and type of charge as well as the dimensions of the charge container. In order to have a relative comparison of severity of the injuries inflicted by AP mines, a series of numerical simulation studies were performed for the entire spectrum of anti-personnel mine threats available worldwide. Four different AP mines were investigated ranging from the one of the world's smallest AP mine M-14 (28 grams of Tetryl) to the world's largest AP mine PMN (240 grams of TNT), including two intermediate level AP landmines: PMA-3 (35 grams of Tetryl) and PMA-2 (100 grams of TNT). PMA-2 and PMN are one of the largest AP mines which can damage victim's entire lower limb frequently requiring above knee amputation. For such extreme loading, it is very difficult to obtain high strain rate data of human tissues to study injuries accurately. Therefore, instead of directly studying injuries, key injury causing blast wave parameters were quantified and compared for various AP mine threats. An understanding the of the blast parameters of the different mines will give an estimate about the damage it can inflict on a human leg or any protective structure.

Blast wave peak over-pressures, velocity and stand-off distance are parameters that play a pivotal role in determining the extent of lower extremity trauma when subjected to anti-personnel (AP) mine blast. Other important parameters such as impulse and energy (kinetic energy) imparted to

the lower limb/protective equipment are secondary variables which can be derived from pressure and velocity respectively. Therefore, for the context of studying the lower limb injuries, it is useful to represent mine blast severity in terms of its key injury causing parameters which are blast wave pressure and velocity.

Fig. 19 (a) represents peak overpressure vs time plots at the soil surface (location of blast wave interaction with the foot location) for the four mines under consideration. All curves follow the Friedlander curve pattern, with a large initial peak that exponentially decays with time. The PMN mine has the highest peak over pressure of 115 MPa, owing to the large amount of the charge (240g TNT), while M-14 mine has the minimum peak overpressure of 13 MPa. A similar trend is observed for the specific impulse as shown in Fig. 19 (b), with the highest specific impulse of 6150 kPa.ms for the PMN mine, and 2500 kPa.ms for PMA-2 mine. M-14 and PMA-3 mines have specific impulse value of 1962 and 2041 kPa.ms respectively.

As presented in Fig. 19 (c), AP mines detonate in soil at pressures of the order of 27000 bar for M-14 mine to 57000 bar for PMN mine. This pressure drops significantly (26bar for M-14 and 60bar for PMN) at a standoff distance of 100mm. The pressure drop with the standoff distance is drastic, however, the absolute pressure near the soil surface (and human foot) is still significantly high (150bar-1100bar). Human bones and soft tissues are not capable of withstanding such extreme loads and get instantly pulverized.

Simulated velocity fringe plots at the location of the victim's foot are presented in Fig. 20. Maximum vertical velocity transmitted to the foot by the AP mines range from 700m/s for an M-14 mine to 1111m/s for the case of PMN mine. Velocity magnitude provide valuable insights into the kinetic energy and momentum transmission into the human foot. Interaction of these extremely high pressures, velocities of blast wave wreak havoc in the vicinity of the foot and give an ad-hoc view of the extreme conditions surrounding the human lower extremity in an AP mine blast event. Table 3 shown below summarizes the blast parameters for the four mines.

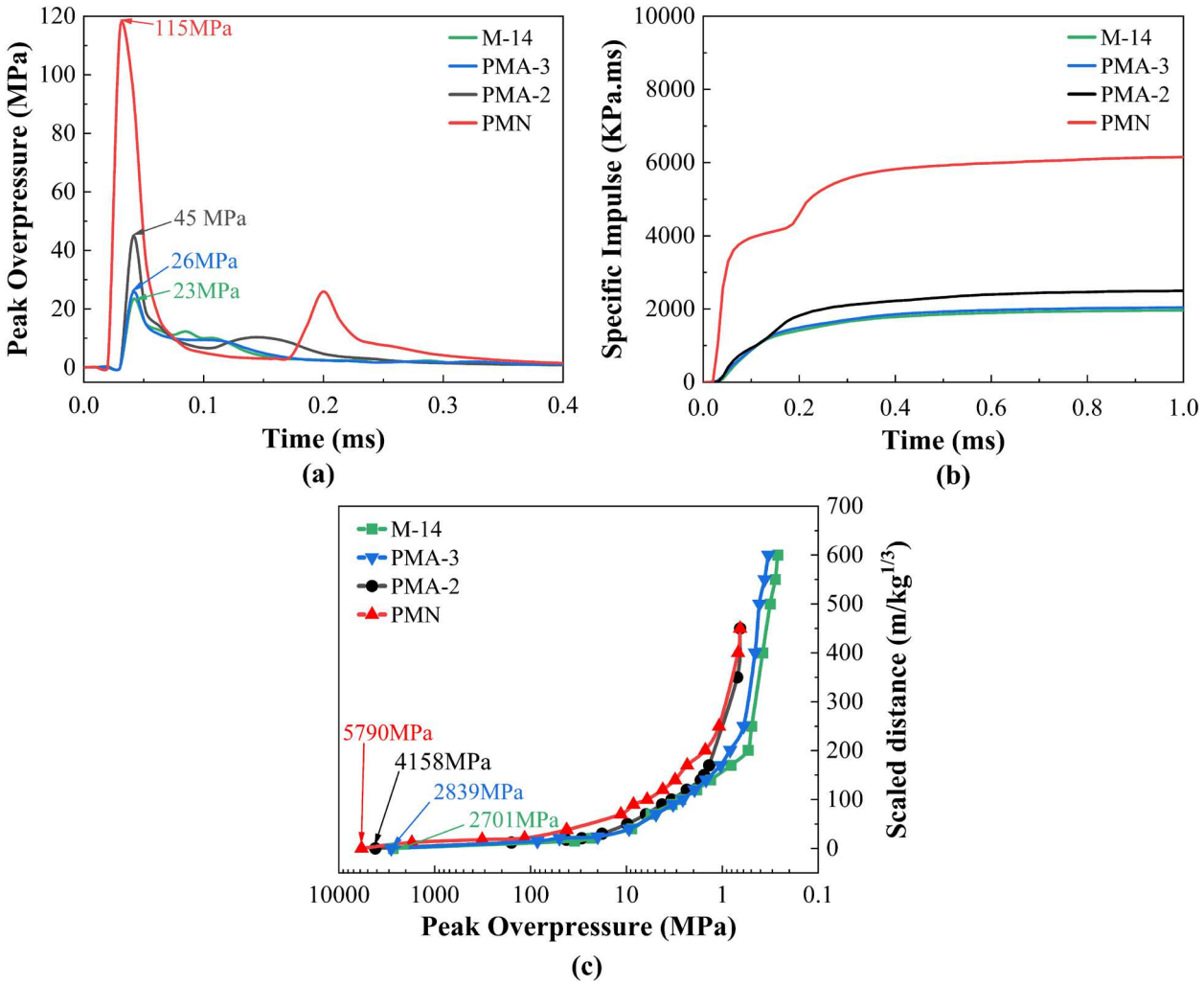

Fig. 19 Comparison of key injury causing parameters plotted for the entire range of AP mine threats available worldwide (a) Peak overpressures (b) Specific impulse comparison at the location of the air-soil interfacial location of the foot, (c) Peak overpressures reduction over various scaled distances

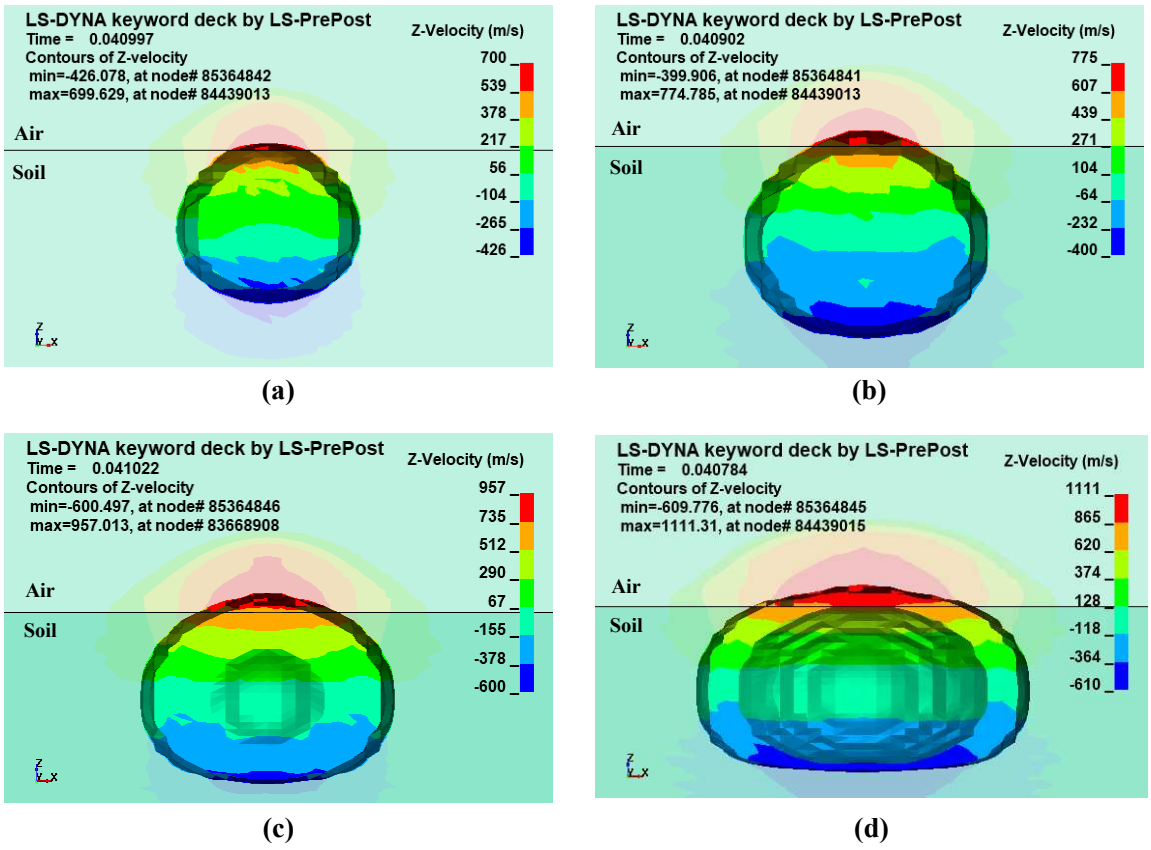

Fig. 20 Velocity fringe plots depicting the peak velocity at the instant when blast wave has just protruded soil-air interface, at the impact location with the foot for (a) M-14 (b) PMA-3 (c) PMA-2 and (d) PMN mines

Table 2 Comparison of blast parameters for M-14, PMA-2, PMA-3 and PMN mines

Mine	Amount of charge (g)	Peak over pressure (MPa)		Instantaneous Velocity (m/s)		Mach No.
		30 mm Stand-off distance	50 mm Stand-off Distance	1st instant	2nd Instant	
M-14	28 (Tetryl)	23	7.8	663	650	1.93
PMA-3	35 (Tetryl)	26	8.3	747	698	2.18
PMA-2	100 (TNT)	45	16	930	884	2.71
PMN	240 (TNT)	115	76	1040	974	3.03

3.4 Blast mitigation strategies

As discussed in the previous sections, AP mine blast causes serious injuries to the leg, and hence it is necessary to study suitable protective measures to mitigate the extent of the trauma. For designing blast protective footwear, there are various methodologies by which the load transmitted to the leg can be reduced sufficiently to avoid injuries to the leg [36]. First method involves increasing the distance between the structure and the detonation point of the explosive (standoff distance). This results in an increase in the time of arrival and decrease in the intensity of the blast wave and hence the force transmission also decreases. Second strategy is to use blast-mitigating materials which can absorb a portion of energy from the blast and reduce the force transmitted to the structure. The energy absorption mechanism can differ for different material. For instance, metals absorb energy by plastic deformation, whereas composites absorb energy by delamination and fiber breakage. Third strategy can be to deflect the blast wave with the help of a deflector plate with an appropriate angle of deflection. The position of the deflector plate with the respect to the detonation point plays a major role and hence in some cases it has been found out that the force gets amplified instead of getting reduced [37]. The fourth strategy is off-axis strategy and used in spider boots, where the point of detonation is at some distance from the axis of leg, due to which a small portion of the wave strikes the leg and induces damage. The current study uses the second strategy and investigates different combination of blast-mitigating materials to compare their damage reducing capabilities. A mine protective shoe concept shown in Fig. 21 was realized using an energy dissipating material (Aluminum foam) placed as an insert in the natural rubber shoe. The insert space as shown in Fig. 21 is filled with aluminum foam sandwiched between aluminum facesheets in double and single core configurations. The configurations vary in terms of their core thickness, face sheet thickness and are collectively shown in Table 4, where M and NM refers to mitigated and non-mitigated scenarios, respectively. The letter after the dot represents the position of explosive (H=Heel, M=Middle, F=Front). For this study, the shoe is kept below the foot and at the soil surface.

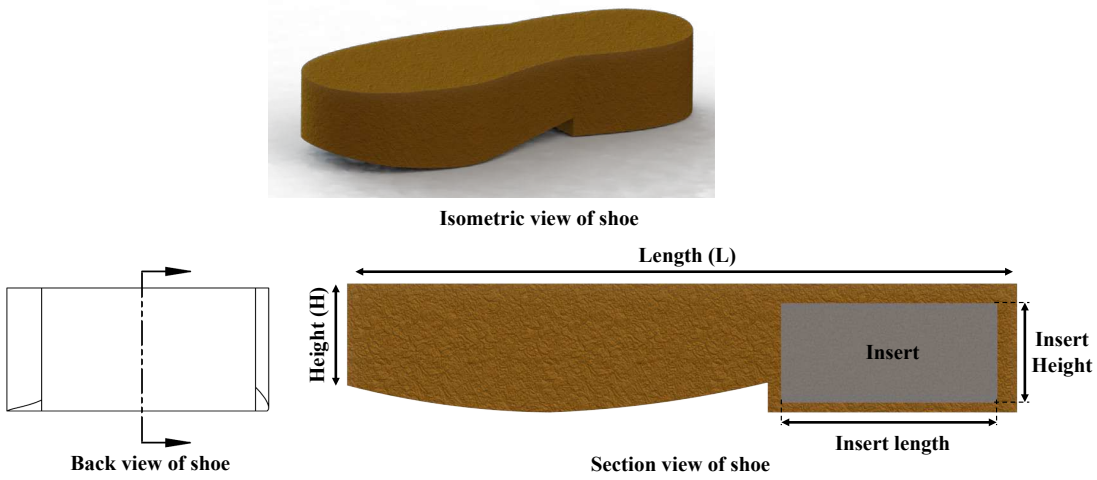

Fig. 21 Different of views of the show with insert

The rubber used for the shoe is natural rubber and is modeled using Mooney-Rivlin hyperelastic constitutive model. The coefficients C_{10} and C_{01} are 5.6 and 0.5 are obtained by curve fitting the stress vs strain curve of natural rubber at 4000 s^{-1} taken from the SHPB experiments done by Khodadadi et al [38]. Cellular materials such as honeycomb and foam are considered to be excellent blast mitigating materials. They absorb energy by progressive buckling of cell walls, and the compression of air trapped inside the hollow portion of the material. Aluminum foams are 3D cellular structures, that contains non-uniform pores in the material and are used as core material in sandwich composite panels to protect civil structures [39]–[41]. Therefore, for high energy absorption, the core material in the insert combinations is taken as Aluminum foam. Aluminum honeycombs have been used in the past for energy absorption from blast impact however, in case of blast impact there may be a chance of fragments flying off and resulting in secondary injuries to the other leg of the victim or nearby army personnel. In addition, the Total Energy Absorption (TEA) of aluminum honeycombs is less than that of aluminum foams. Therefore, aluminum foam outweighs aluminum honeycomb in terms of TEA and fragments. Strain rate dependent material properties for the Aluminum foam are taken from the study done by Novak et al. [42]. Novak et al. [42] conducted quasistatic and high strain rate compression tests (using SHPB) on Aluminum foam upto a strain rate as high as 12000/s. Literature shows that the energy absorption in metallic foams increases with increasing relative density, therefore

the aluminum foam with a high density of 681 kg/m^3 is taken as the core material. Aluminum foam cores of 20 mm and 30 mm thickness were considered for the study, as these thickness have shown good mitigation capabilities in blast scenarios [39], [43].

Aluminum alloy Al-5005 is taken as the material for the face sheets (mass density 2680 kg/m3, yield stress 318 MPa, Young's modulus 72 GPa, and tangent modulus 737 MPa) [44]. The mechanical behavior of the face sheets is governed by material model Piecewise Linear Plasticity model, which is a bi-linear elasto-plastic constitutive model. The face sheet thickness of 5 mm gives better results compared to the 2.5 mm which can be attributed to the stiffness of the core, here aluminum foam. Higher density of foam has higher stiffness and hence requires high amount of force to get compressed. In our case, density of 681 kg/m^3 (relative density = 0.25) is used which is on the higher side, therefore face sheets of 5 mm thickness give better results.

For modeling the aluminum foam, MAT_MODIFIED_CRUSHABLE_FOAM material model was used in LS-Dyna software. This model is specifically designed for crushable foams with optional cards to give damping, tension cut-off and strain rate dependent material properties. This material card is a modified version of MAT_CRUSHABLE_FOAM. Rate dependent material properties can be accounted by giving a table of curves, with each curves representing the volumetric stress versus strain for a particular strain rate.

For intermediate strain rate levels, properties are determined by interpolating between the given curves bounding the strain rates. The identified parameters for the aluminum foam are in Table 5. Fig. 22 shows the experimental curve (High strain rate and quasi static) of the Aluminum foam of density 681 kg/m^3. To validate the properties of aluminum foam, quasistatic and high strain rate compression simulations were conducted, and the stress vs strain response was compared to the experimental which showed good correlation as shown in Fig. 22.

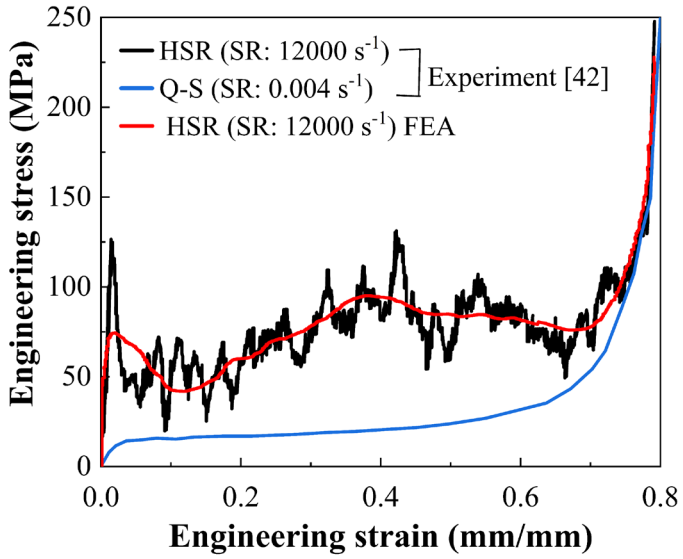

Fig. 22 Strain dependent quasistatic (0.004/s) and high strain rate (12000/s) material properties of aluminum foam

The deformation pattern before and after blast impact for M.H.1 is depicted in Fig. 23. It can be seen that the complete densification of both aluminum foam cores does not occur. The blast wave strikes the bottom face sheet, resulting in curvature deformation of the face sheet and the deformation shape is replicated in the bottom aluminum foam core. The major deformation happens at the center of the foam, where the Aluminum foam is compressed from 30 mm to 8.2 mm. The middle face sheet does not deform instead it plays the role of uniformly compressing the top aluminum foam core from 30 mm to 9.1 mm.

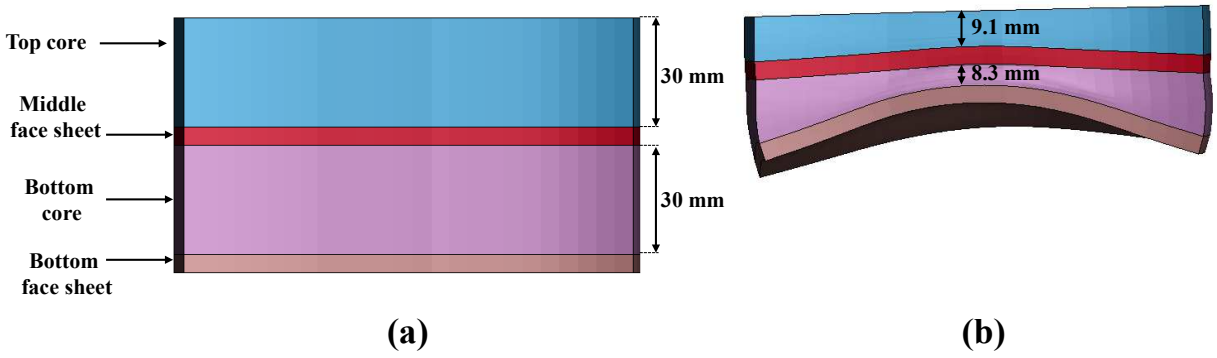

Fig. 23 (a) Before impact and (b) After impact scenario for configuration MH1 mitigation

Table 3 Blast mitigation combinations and results

Case	Configuration	Core Thickness	Facesheet Thickness (mm)	Tibia Section Peak force (kN)		Impulse to Tibia (Ns)		
				Value	% Reduction	Value	% Reduction	Total energy absorbed by insert (J)
Heel Detonation								
NM.H	**Benchmark**			**13.2**		**9.15**		**-**
M.H.1	Double core	30 mm	5	8.67	34.3	7.15	21.9	5300
M.H.2	Double core	20mm	5	8.96	32.1	7.78	15	5060
M.H.3	Double core	30 mm	2.5	9.46	28.3	7.33	19.9	4650
M.H.4	Single core	40 mm	5	9.6	27.3	7.14	22	4503
Combat boot				12.0	9.1			
Middle Detonation								
NM.M	**Benchmark**			23.1		14.84		
M.M	Double core	30 mm	5	13.8	40.3	13.16	11.3	5760
Front Detonation								
NM.F	**Benchmark**			13.8		14.2		
M.F	Double core	30 mm	5	5.48	60.3	10.9	23.2	5160

Table 4 Identified parameters for MAT_163 material model for Aluminum foam

Property	Value
Density of foam (kg/m^3)	681
Elastic modulus (MPa)	5024
Poisson's ratio foam	0.11
SRFLAG	1

The results are discussed focusing on the behavior of the insert materials since the rubber material surrounding the insert material is for structural integrity and plays only a small role in mitigating the force. In reality, rubber materials become stiffer and transit into brittle behavior under high strain rate loading and fail at lower strain rate [38]. When the explosive interacts with

the rubber its primary function is to transfer the load to the cellular structure (here, Aluminum foam sandwich panel) that will absorb energy. This behavior was noted by blast experiments on boot or shoe [45].

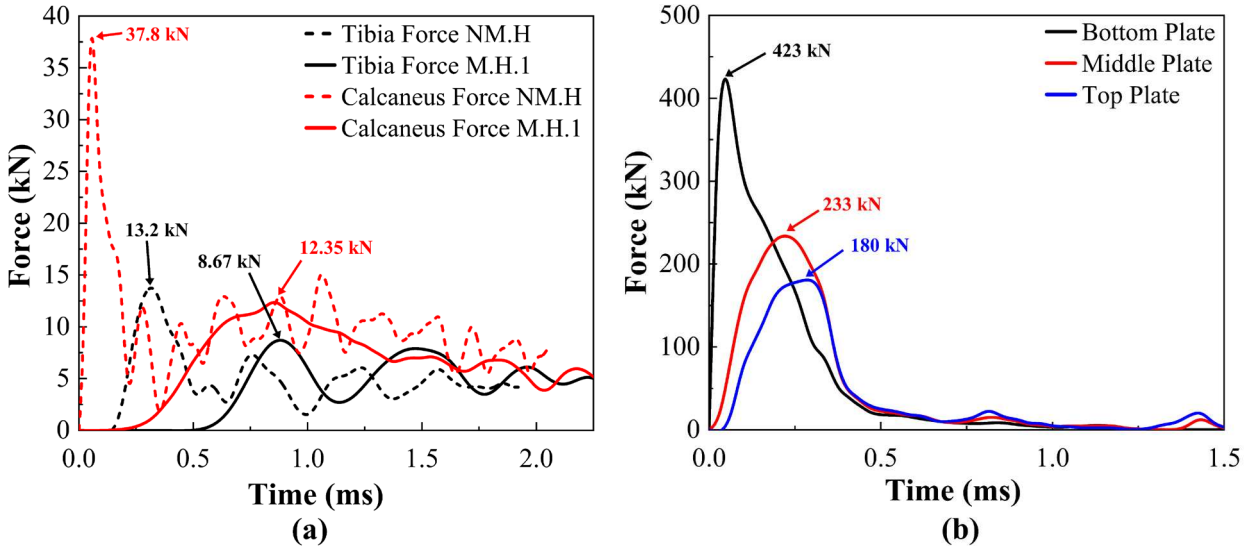

Fig. 24 Force vs time for (a) heel detonation Mitigation vs Non-mitigation (b) Force transmission for MH.1 (Mitigation Heel- scenario-1) configuration

Fig. 24 (a) shows the effect of using MM.1 shoe insert configuration on mitigating calcaneus and Tibia forces for heel detonation. The peak calcaneus force decreases by 67% and there is a decrease of 34% for the tibia force. The peak section force in the tibia and the total impulse for all the configurations are compared in Table 4. It was observed that for all the configurations the peak section force measured in tibia is less in case where mitigation strategy is implemented compared to the barefoot scenario. In case of metallic foams as core material, care should be taken in selecting the height of the core so that complete densification does not happen and at the same time foam is compressed to a certain level such that it absorbs energy from the blast impact. At densification, the cell walls collapse and the porous material gets compressed to a flat plate, which has shown to increase the force transmission in some cases [39]. As shown in Fig. 24 (b), the force gets reduced progressively as the blast wave passes through the blast mitigation materials. At the bottom plate, a force of 423 kN is obtained which is reduced to 233 kN at the

middle plate and finally to 180 kN at the top plate. On comparing the MH.2 and MH.3 cases, it was observed that in comparison to the single core sandwich panel, double core combination was able to mitigate the force by an additional 1kN. This is because in single layer, complete compression of aluminum foam does not take place owing to the high stiffness of the high thickness foam, resulting in incomplete utilization of the cellular material. Whereas, in case of double core configuration, both bottom and top aluminum foam crush separately resulting in more energy absorption. To study the effect of face sheet thickness, M.H.1 and M.H.3 configurations were compared, and it was observed that with 5 mm thickness face sheets were able to crush the aluminum foam more compared to the 2.5 mm thickness hence, resulting in more mitigation (22% more reduction of peak tibia force).

Comparison of the proposed mitigation concept with the standard combat boot used by army personnel is shown in Fig. 25. It was observed that the current mitigation strategy reduces the peak tibia force by 4.53 kN, whereas the combat boot only attenuates the peak tibia force by 1.2 kN. Therefore, the designed protective shoe with aluminum foam sandwich panels provides an additional force mitigation of around 25.2% than army combat boots.

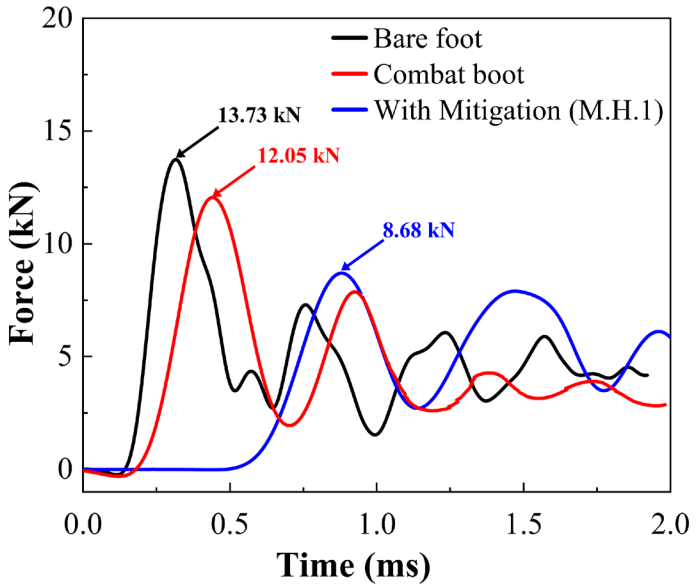

Fig. 25 Comparison of M.H.1 mitigation scenario with combat boot

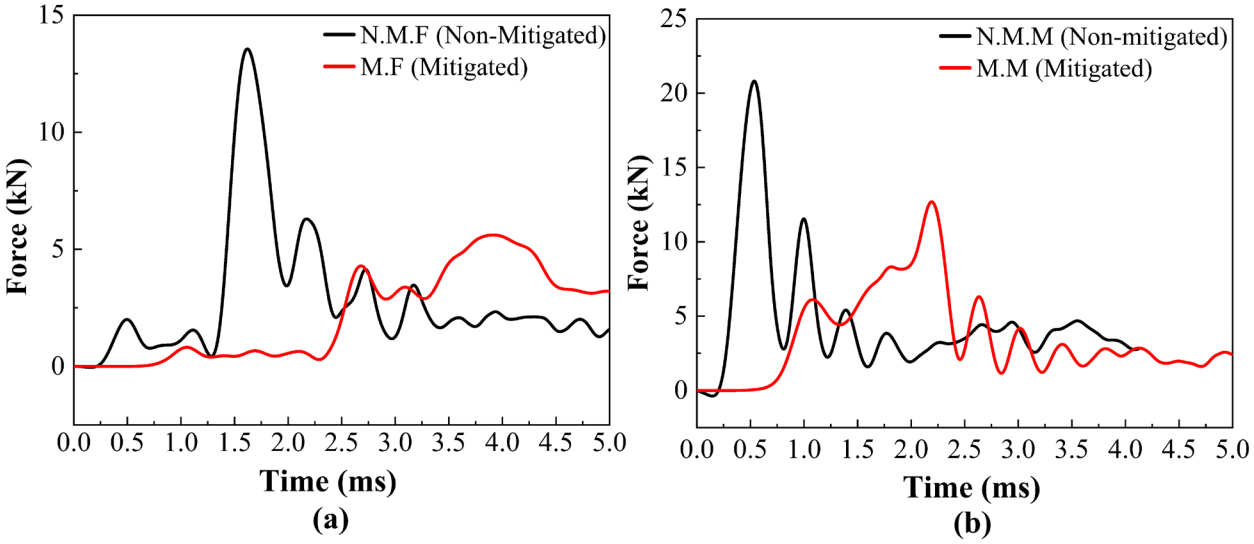

Fig. 26 Force vs time for (a) Front and (b) middle detonation

As discussed in above sections, the position of foot which triggers the mine detonation plays a crucial role in determining the extent of damage to the foot. Therefore, in addition to the heel position, FE simulations for mitigation were conducted for front and middle position taking the configuration (M.H.1) that gave the best mitigation in case of heal detonation. As shown in Fig. 26 (a), due to the front position of the explosive, the peak force gets delayed compared to the heel detonation, and in the presence of the protective shoe, the peak force is reduced to 5.48 kN (60% reduction) and delayed even further. According to the study done by Dong et al. [43], the minimum force required for tibia fracture is 8.5 kN in the case of deck slap injuries (vehicle floor plate impact) on the mounted military personnel caused by an antivehicle mine blast. In the presence of blast mitigation material in the form of sandwich structure, the scenario becomes similar to the floor impact condition, with the bottom plate transmitting the load to the foot. Therefore, from the analysis results it follows that with the use of proposed protective footwear, victim can escape with minor damage to the tibia under hind-foot detonation while for front-foot detonation of M-14 mine detonation, no tibia damage is expected.

4 Conclusions

This paper has described a plausible injury mechanism of the lower limb under M-14 mine blast based on the simulation of the event corroborated with cadaver test data. To study near-field trauma on the lower limb, simulations were performed to develop a reference mine blast computational framework based on validation of a 100-gram C-4 landmine detonated in soil. Soil crater width and detonation cloud height were correlated with test data (max error margin of 4.8%). The dimensions of the soil crater dominate how the blast wave will be reflected and directed towards the victim. Good correlation was obtained for in-air and in-soil pressures for very close-field scaled distances (0.19m/kg$^{1/3}$) making the developed mine blast framework feasible for studying the near-field foot trauma due to direct interaction with a landmine. A novel Finite Element framework with THUMS^{TM} model was validated against two series of cadaver test data for M-14 detonation under the heel. Model predictions agreed well with the cadaver test data in terms of peak force and time of the arrival of peak. The tibia forces were predicted to be 13.5 kN for bare foot with 3.3% error and 11.4 kN for combat boot with 3.5% error). Using this validated high fidelity FEM framework, the main conclusions of this research paper are summarized below:

(1) Deep buried landmines were found to have a wider crater than shallow buried mine, providing large opening area for release of the blast detonation products, however the peak overpressures reduced significantly with increasing DOB. For a 100 gram C-4 mine, Peak in-air pressure at a standoff of 300mm above ground was found to be 4.29MPa for a landmine flush with the ground. This peak overpressure reduces to 1.38MPa for mine burial depth of 30mm which subsequently reduced to 0.79MPa when DOB of the mine is increased to 80mm.

(2) M-14 mine blast detonation causes an in-soil peak pressure of 2701MPa at around 9.8 microseconds. Reflected blast wave reaches the soil-air interface at a peak pressure of 22MPa in around 86 microseconds, eventually bursting the soil cap to expel the detonation products towards the victim. Pressure eventually reduces to atmospheric pressure which indicates that the M-14 mine blast phenomenon lasts only 1millisecond.

(3) A parametric study carried out by varying the mine detonation location along the foot, revealed that the tibia force (20kN) was maximum for mid-foot detonation of the M-14

mine which shows that it is the most critical scenario and must be considered while designing appropriate protective equipment. This observation is supported by the finding that the maximum FSI force (500 kN) is experienced for mid-foot detonation, due to the blast wave directly interacting with a larger portion of foot.

(4) For an M-14 mine explosion triggered by the hind-foot of the victim, level of protection offered by a military standard combat boot was assessed. For an M-14 mine blast, a meindl military combat boot was found to reduce the tibia force of 13.2kN for a bare foot scenario to 12.05kN.

(5) For mitigating the lower limb trauma, a proposed protective shoe concept with single and double layer configurations of aluminum foam sandwich structure as shoe inserts were studied by varying the core and facesheet thickness. Aluminum foam with density 681 kg/m^3 (sandwiched between aluminum alloy Al-5005 facesheets) was taken for the study due to its high specific energy absorption. Strain dependent material properties were used for aluminum foam ranging from quasi-static strain rate of 0.004/s to high strain rates as high as 12000/s. Results showed that for heel detonation of M-14 mine, this proposed protective shoe concept was effective in reducing the peak tibia force from 13.02kN (bare foot) to 8.68kN (34.3% reduction). Impulse transferred reduced from 9.15Ns (bare foot) to 7.15Ns (21.9% reduction). Comparison between double and single core combination of aluminum foam depicted that double core configuration in sandwich configuration, is more efficient in absorbing energy. The same configuration also demonstrated higher mitigation capabilities in mid-foot and front-foot detonation reducing the peak tibia force by 40.3% and 60.3% respectively.

Numerical biological models for analyzing the blast effects on human lower limb have various limitations. Most of the existing high strain characterization of bones has been done using animal bones taken from bovine and goat subjects. Despite using animal test data from literature, reasonable agreement has been numerically correlated with human cadaver mine blast test data. Key injury parameters were investigated instead of directly studying lower limb injuries for mines with higher charge content because of the unavailability of high strain rate data for such extreme conditions. For future work, elaborate in-situ cadaveric testing is required for human lower limb musculoskeletal tissues for improving the model biofidelity. Furthermore, additional

energy absorbing cellular materials could be investigated for further lowering the load transmission.

Declaration of conflicting interests

The author(s) declared no potential conflicts of interest with respect to the research, authorship and/or publication of this article.

Author Contributions

Baljinder Singh: Conceptualization, Methodology, Software, Validation, Formal analysis, Investigation, Data curation, Writing-original draft and editing, visualization. **Mohammad Ahmed Basri:** Methodology, Software, Validation, Formal analysis, Investigation, Data curation, Writing-original draft and editing, visualization.

Acknowledgments:

The authors thankfully acknowledge the Defence Research & Development Organisation for funding the project vide grant #ERIP/ER/1600495/M/01/1678.

References

[1] "75/52 Implementation of the convention on the prohibition of the use, stockpiling, production and transfer of anti personnel mines and on their destruction," 2021.

[2] D. S. Cronin *et al.*, "Test methods for protective footwear against AP mine blast," 2003.

[3] C. G. Coffey, K. Torrance, D. Lonson, and others, "Design, construction and commissioning of a surrogate human leg test facility," *Amtech Rep. TR9775*, vol. 2701, 1999.

[4] J. van Bree, "HFM/ET007 Position paper," 2000.

[5] D. Bourget, G. Pageau, K. V Williams, and D. S. Cronin, "AP Mine Blast Effects on Surrogate Lower Leg," 2000.

[6] K. Williams, D. Bourget, D. Cronin, D. Bergeron, and C. Salisbury, "Simplified biofidelic lower leg surrogate." Google Patents, 2006.

[7] M. J. Footner, D. M. Bergeron, and R. J. Swinton, “Development and calibration of a frangible leg instrumented for compression and bending,” 2006.

[8] D. M. Bergeron, G. G. Coley, R. W. Fall, and I. B. Anderson, “Assessment of Lower Leg Injury from Land Mine Blast--Phase 2,” *Def. Res. Dev. Canada*, pp. 2007–2070, 2007.

[9] R. M. Harris, M. S. Rountree, L. V Griffin, R. A. Hayda, and T. Bice, “Final Report of the Lower Extremity Assessment Program (LEAP 99-2). Volume 2,” 2000.

[10] R. Harris *et al.*, “The effects of antipersonnel blast mines on the lower extremity,” 1999.

[11] Denis Bergeron; Clay Coffey; Robert Walker; Defence Research Establishment Suffield, “Detonation of 100-gram anti-personnel mine surrogate charges in sand : a test case for computer code validation.” .

[12] J. Wang, “Simulation of a landmine explosion using LS-DYNA3D software: Benchmark work of simulation of explosion in soil and air,” 2001.

[13] J. Motuz, D. S. Cronin, M. Worswick, D. Bourget, K. Williams, and G. Pageau, “Numerical Modelling of a Simplified Surrogate Leg Subject To an Anti-Personnel Blast Mine,” in *International Symposium of Ballistics*, 2011, vol. 19.

[14] Denis Bergeron 1998, “Detonation of 100-gram anti-personnel mine surrogate charges in sand : a test case for computer code validation.” .

[15] C. Fichera, L. Peroni, and M. Scapin, “Numerical simulation of landmine explosions: comparison between different modelling approaches,” in *COUPLED V: proceedings of the V International Conference on Computational Methods for Coupled Problems in Science and Engineering:*, 2013, pp. 708–719.

[16] D. M. Bergeron, I. B. Anderson, C. G. Coley, and R. W. Fall, “Assessment of Lower Leg Injury from Land Mine Blast--Phase 1: Test Results using a Frangible Surrogate Leg with Assorted Protective Footwear and Comparison with Cadaver Test Data,” *DRDC Suff. TR*, vol. 51, 2006.

[17] R. Bertucci *et al.*, “An Anatomically-Relevant Computational Model for Primary Blast Effects on the Human Lower Extremity,” *J. Mech. Med. Biol.*, vol. 18, no. 06, p. 1850057, 2018.

[18] E. G. Pickering, S. Chung Kim Yuen, G. N. Nurick, and P. Haw, “The response of quadrangular plates to buried charges,” *Int. J. Impact Eng.*, 2012, doi:

10.1016/j.ijimpeng.2012.05.007.

[19] Y. Kitagawa, H. Ichikawa, A. I. King, and R. S. Levine, “A severe ankle and foot injury in frontal crashes and its mechanism,” 1998, doi: 10.4271/983145.

[20] P. Schreiber, J. Crandall, S. Hunvitz, and G. S. Nusholtz, “Static and dynamic bending strength of the leg,” *Int. J. Crashworthiness*, 1998, doi: 10.1533/cras.1998.0077.

[21] J. Kajzer, G. Schroeder, H. Ishikawa, Y. Matsui, and U. Bosch, “Shearing and bending effects at the knee joint at high speed lateral loading,” 1997.

[22] M. Lalwala, A. Chawla, P. Thomas, and S. Mukherjee, “Finite element reconstruction of real-world pedestrian accidents using THUMS pedestrian model,” *Int. J. Crashworthiness*, 2020, doi: 10.1080/13588265.2019.1594547.

[23] Z. Asgharpour, P. Zioupos, M. Graw, and S. Peldschus, “Development of a strain rate dependent material model of human cortical bone for computer-aided reconstruction of injury mechanisms,” *Forensic Sci. Int.*, 2014, doi: 10.1016/j.forsciint.2013.11.010.

[24] J. H. McElhaney, “Dynamic response of bone and muscle tissue.,” *J. Appl. Physiol.*, 2017, doi: 10.1152/jappl.1966.21.4.1231.

[25] T. P. M. Johnson, S. Socrate, and M. C. Boyce, “A viscoelastic, viscoplastic model of cortical bone valid at low and high strain rates,” *Acta Biomater.*, 2010, doi: 10.1016/j.actbio.2010.04.017.

[26] Livermore Software Technology Corporation (LSTC), *LS-DYNA® Keyword User’s Manual – Volume II – Material Models – R9.0*. 2016.

[27] B. Singh, D. K. Dubey, A. Chawla, and S. Mukherjee, “Failure Analysis of Human Lower Extremity During Lateral Blast: A Computational Study,” *Compos. Mater. Extrem. Load.*, p. 355.

[28] J. O. Hallquist and others, “LS-DYNA keyword user’s manual,” *Livermore Softw. Technol. Corp.*, vol. 970, pp. 299–800, 2007.

[29] J. Shin, A. S. Whittaker, and D. Cormie, “Incident and Normally Reflected Overpressure and Impulse for Detonations of Spherical High Explosives in Free Air,” *J. Struct. Eng.*, 2015, doi: 10.1061/(asce)st.1943-541x.0001305.

[30] K. Vasilis, S. George, and L. Martin, “VALIDITY OF BLAST PARAMETERS IN THE NEAR-FIELD.”

[31] C. N. Kingery and G. Bulmash, “Technical report ARBRL-TR-02555: Air blast parameters from TNT spherical air burst and hemispherical burst, AD-B082 713,” *US Army Ballist. Res. Lab. Aberdeen Proving Ground, MD*, 1984.

[32] N. Newell, R. Salzar, A. M. J. Bull, and S. D. Masouros, “A validated numerical model of a lower limb surrogate to investigate injuries caused by under-vehicle explosions,” *J. Biomech.*, vol. 49, no. 5, pp. 710–717, 2016, doi: 10.1016/j.jbiomech.2016.02.007.

[33] I. Chant, D. Lee, and D. Ireland, “DSTO landmine detection test targets,” 2005.

[34] B. M. Dobratz, “Properties of chemical explosives and explosive simulants,” *Lawrence Livermore Natl. Lab.*, 1972.

[35] E. A. Nečaev, *Mine blast trauma: Experience from the war in Afghanistan*. Russian Ministry of Public Health and Medical Industry.

[36] R. M. Harris, M. S. Rountree, T. Bice, and S. J. Mannion, “Ada409059,” vol. II, no. 8, 2000.

[37] E. S. M. J. L. Fujinaka, “Research and development of blast protective footwear, fabrication and prooftesting,” p. 117 p., 1966.

[38] A. Khodadadi, G. Liaghat, D. Shahgholian-ghahfarokhi, M. Chizari, and B. Wang, “Thin-Walled Structures Numerical and experimental investigation of impact on bilayer aluminum-rubber composite plate,” vol. 149, no. February, 2020.

[39] F. Zhu, L. Zhao, G. Lu, and Z. Wang, “Structural response and energy absorption of sandwich panels with an aluminium foam core under blast loading,” *Adv. Struct. Eng.*, vol. 11, no. 5, pp. 525–536, 2008.

[40] C. Wu, L. Huang, and D. J. Oehlers, “Blast Testing of Aluminum Foam–Protected Reinforced Concrete Slabs,” *J. Perform. Constr. Facil.*, vol. 25, no. 5, pp. 464–474, 2011, doi: 10.1061/(asce)cf.1943-5509.0000163.

[41] H. Liu, Z. K. Cao, G. C. Yao, H. J. Luo, and G. Y. Zu, “Performance of aluminum foam-steel panel sandwich composites subjected to blast loading,” *Mater. Des.*, vol. 47, pp. 483–488, 2013, doi: 10.1016/j.matdes.2012.12.003.

[42] L. Jing, X. Su, F. Yang, H. Ma, and L. Zhao, “Compressive strain rate dependence and constitutive modeling of closed-cell aluminum foams with various relative densities,” *J. Mater. Sci.*, vol. 53, no. 20, pp. 14739–14757, 2018, doi: 10.1007/s10853-018-2663-z.

[43] L. Dong *et al.*, “Blast effect on the lower extremities and its mitigation: A computational study,” *J. Mech. Behav. Biomed. Mater.*, vol. 28, pp. 111–124, 2013, doi: 10.1016/j.jmbbm.2013.07.010.

[44] W. Li, G. Huang, Y. Bai, Y. Dong, and S. Feng, “Dynamic response of spherical sandwich shells with metallic foam core under external air blast loading - Numerical simulation,” *Compos. Struct.*, vol. 116, no. 1, pp. 612–625, 2014, doi: 10.1016/j.compstruct.2014.05.038.

[45] M. Karahan, E. A. Karahan, and N. Karahan, “Blast Performance of Demining Footwear: Numerical and Experimental Trials on Frangible Leg Model and Injury Modeling,” *J. Test. Eval.*, vol. 46, no. 2, pp. 666–679, 2017.

Supplementary Files

This is a list of supplementary files associated with this preprint. Click to download.

- Supplementary.docx